



# Fine-scale fluctuations of PM<sub>1</sub>, PM<sub>2.5</sub>, PM<sub>10</sub> and SO<sub>2</sub> concentrations caused by a prolonged volcanic eruption (Fagradalsfjall 2021, Iceland)

Rachel C. W. Whitty<sup>1</sup>, Evgenia Ilyinskaya<sup>1</sup>, Melissa A. Pfeffer<sup>2</sup>, Ragnar H. Thrastarson<sup>2</sup>, Þorsteinn Johannsson<sup>3</sup>, Sara Barsotti<sup>2</sup>, Tjarda J. Roberts<sup>4, 5</sup>, Guðni M. Gilbert<sup>2, 9</sup>, Tryggvi Hjörvar<sup>2</sup>, Anja Schmidt<sup>6, 7, 8</sup>, Daniela Fecht<sup>10</sup>, Grétar G. Sæmundsson<sup>11</sup>

<sup>1</sup>COMET, Institute of Geophysics and Tectonics, School of Earth and Environment, University of Leeds, Leeds, LS2 9JT, United Kingdom

<sup>2</sup>Icelandic Meteorological Office, 150 Reykjavík, Iceland

<sup>3</sup>The Environment Agency of Iceland, 108 Reykjavík, Iceland

<sup>4</sup>CNRS UMR7328, Laboratoire de Physique et de Chimie de l'Environnement et de l'Espace, Université d'Orléans, Orléans, 45071, France

<sup>5</sup>LMD/IPSL, ENS, Université PSL, École Polytechnique, Institute Polytechnique de Paris, Sorbonne Université, CNRS, F-75005 Paris, France

<sup>6</sup>Yusuf Hamed Department of Chemistry, University of Cambridge, Cambridge, CB2 1EW, United Kingdom

<sup>7</sup>Institute of Atmospheric Physics (IPA), German Aerospace Centre (DLR), 82234 Oberpfaffenhofen, Germany

<sup>8</sup>Meteorological Institute, Ludwig Maximilian University of Munich, 80333 Munich, Germany

<sup>9</sup>Nox Medical, 150 Reykjavík, Iceland

<sup>10</sup>MRC Centre for Environment and Health, School of Public Health, Imperial College London, London, W12 0BZ, United Kingdom

<sup>11</sup>Department of Research and Analysis, Icelandic Tourist Board, 101 Reykjavík, Iceland

*Correspondence to:* Evgenia Ilyinskaya (e.ilyinskaya@leedss.ac.uk)

25

## Abstract.

The 2021 Fagradalsfjall fissure eruption was the first of multiple ongoing eruptions in the most densely populated part of Iceland (70% of population within 50 km). It was monitored by an exceptionally dense reference-grade air quality network (14 stations within 40 km), and the first time that a reference-grade timeseries of PM<sub>1</sub> was collected during an eruption. We 30 used these measurements to investigate fine-scale dispersion patterns of volcanic air pollutants (SO<sub>2</sub>, PM<sub>1</sub>, PM<sub>2.5</sub>, PM<sub>10</sub>) in populated areas.



Despite its small size the eruption caused a statistically-significant increase in average and peak PM and SO<sub>2</sub> concentrations in at least 300 km distance. Peak daily-means of PM<sub>1</sub> peak rose to 18-20 µg/m<sup>3</sup> from 5-6 µg/m<sup>3</sup>; and proportion of PM<sub>1</sub> increased relative to coarser PM fractions (21-24% of PM<sub>10</sub> compared to 14% background). Eruption increased PM<sub>10</sub> and 35 PM<sub>2.5</sub> by ~50% in populated areas with low background concentrations, but its impact was not measurable in areas with high background sources. This suggests that ash-poor eruptions are one of, or the most, important source of PM<sub>1</sub> in Iceland, and potentially in other areas exposed to volcanic emissions.

There were significant fine-scale temporal ( $\leq 1$  hour) and spatial ( $< 1$  km) fluctuations in volcanic pollutant concentrations. In 40 Reykjavík, two stations located  $< 1$  km of each other recorded peak hourly-mean concentrations of 480 and 250 µg/m<sup>3</sup> SO<sub>2</sub>, and 5 and 0 exceedance events, respectively, within a  $\sim 12$ -hour plume advection event. This has implications for population exposures estimates.

## 1 Introduction

Globally, over a billion people are estimated to live within 100 km of an active volcano (Freire et al., 2019), a distance 45 within which they might be exposed to volcanic air pollution (Stewart et al., 2021), and the number of potentially exposed people is growing because of building expansion into previously uninhabited areas near volcanoes. Basaltic fissure eruptions happen frequently near populated areas, for example at Kīlauea volcano on Hawaii (tens of episodes since 1983), Cumbre Vieja on La Palma 2021 and currently on Reykjanes, Iceland (from 2021 and ongoing at the time of writing). Even small, 50 ash-poor fissure eruptions can cause severe air pollution episodes when they happen at the urban interface (Whitty et al., 2020).

Throughout this work, we will refer to ‘volcanic emissions’, and unless otherwise stated, our intended meaning is SO<sub>2</sub> gas 55 and PM (primary and secondary), collectively. Prior to this study, the best observed and studied impacts of volcanic emissions on air quality came from Kīlauea in Hawaii (in particular the 2018 large fissure eruption), and Holuhraun large fissure eruption 2014-2015 in Iceland. Both of these volcanic sources degraded air quality at distances of hundreds of kilometres during times of activity (Crawford et al., 2021; Gíslason et al., 2015; Ilyinskaya et al., 2017; Schmidt et al., 2015; 60 Whitty et al., 2020). A public health investigation of the Holuhraun eruption showed that it was associated with an increase in register-measured health care utilisation for respiratory disease in Iceland’s capital area 250 km from source (Carlsen et al., 2021a, b). The studies of Kīlauea and Holuhraun 2014-2015 eruptions were based on observations from relatively few and distal air quality stations; the closest reference-grade station to Holuhraun was at  $\sim 90$  km distance, and  $\sim 40$  km distance at Kīlauea. When the reference-grade air quality network on Hawaii was augmented by 16 low-cost SO<sub>2</sub> and PM<sub>2.5</sub> sensors 65 during a two-week campaign in 2018 it was shown that estimates of population exposure to volcanic air pollution can change significantly with a denser sensor network (Crawford et al., 2021). Studies of volcanic plume chemistry in Holuhraun and Kīlauea eruptions have hypothesized that there may be significant fine-scale fluctuations in concentrations and dispersion 70



patterns of volcanic gas and PM, potentially very close to the eruption site (Ilyinskaya et al., 2017, 2021), but this has not yet been observed in the field.

65 Fagradalsfjall 2021 was a small fissure eruption that happened in the most densely populated part of Iceland (>260,000 people or ~70% of the country's population lived within 40 km distance from the eruption site). The studies on Holuhraun 2014-2018 and Kilauea 2018 eruptions made important discoveries about distal air quality impacts of large fissure eruptions (erupted volume >1 km<sup>3</sup>), which took place in relatively sparsely populated areas. Small eruptions (erupted volume from <0.1 up to 1 km<sup>3</sup>) are very important to investigate with regards to air pollution because they account for ~80% of eruptions

70 worldwide (Siebert et al., 2015), and their impact on populated areas is likely to increase as the global population grows.

Fagradalsfjall 2021 presented a unique opportunity to advance our understanding of the intensity and dispersion patterns of volcanic air pollution in downwind populated areas. It was monitored by the densest reference-grade air quality monitoring network of any volcano in the world (to our knowledge) with 27 stations across Iceland, thereof 14 stations within 40 km distance from the eruption site. Some of these stations were located within 1 km from one another. This allowed our  
75 investigation into very fine-scale changes in spatial and temporal air quality impacts with respect to sulphur dioxide (SO<sub>2</sub>), and different particulate matter size fractions (PM<sub>1</sub>, PM<sub>2.5</sub>, PM<sub>10</sub>), which are the volcanic air pollutants that are likely to be elevated, both at source and at significant distances downwind (Stewart et al., 2021).

This is also the first study reporting on a reference-grade timeseries of PM<sub>1</sub> during a volcanic eruption. PM<sub>1</sub> is known to be the dominant size fraction in volcanic emissions when measured directly at the volcanic source, but it has never been  
80 measured in downwind populated areas impacted by a volcanic eruption. Evidence-based air quality thresholds have been defined for SO<sub>2</sub>, PM<sub>2.5</sub> and PM<sub>10</sub> but not yet for PM<sub>1</sub>, largely due to the paucity of reference-grade data on concentrations and dispersion (World Health Organization, 2021). PM<sub>1</sub> is only recently being introduced in operational air quality monitoring worldwide (from 2020 in Iceland) and evidence-based guidelines for its levels are not yet established. Available studies unequivocally demonstrate a correlation between increased concentrations of PM<sub>1</sub> and negative health outcomes  
85 (Chen et al., 2017; Wang et al., 2011; Yang et al., 2018) and high-quality datasets on levels and variability of PM<sub>1</sub> are therefore important steps towards establishing air quality guidelines.

## 1.1 Fagradalsfjall 2021 eruption description

Fagradalsfjall 2021 (19 March - 19 September 2021) was the first eruption to happen in the most densely populated area of Iceland in ~800 years, and is considered to have been the beginning of a prolonged eruptive period on the Reykjanes  
90 peninsula, locally known as Reykjanes Fires. At the time of writing, there have been 9 further eruptions on Reykjanes peninsula, thereof two in the Fagradalsfjall volcanic system (August 2022 and July 2023), and seven in the adjacent Reykjanes-Svartsengi system (December 2023 – November 2024). Magma accumulation currently continues and based on the eruption history of the Reykjanes peninsula, eruptive episodes activity may occur repeatedly for decades or centuries. Fagradalsfjall 2021 was a small eruption (total ~0.3 to 0.9 Mt SO<sub>2</sub>, 4.82 km<sup>2</sup> lava (Barsotti et al., 2023; Pfeffer et al., 2024))  
95 but due to its location and population growth it may have exposed more people to volcanic air pollution than any previous



eruption in the country (Fig. 1). The eruption behaviour was very dynamic, and the number of active craters and the eruptive style changed several times during its duration; for further details see (Barsotti et al., 2023).

The eruption site was at 9 km distance from the closest town of Grindavík; and over 70% of Iceland's total population (263,000 out of 369,000 people) lived within 50 km distance, including the capital area of Reykjavík. The easily accessible site was also visited by ~300,000 people for sightseeing during its course.

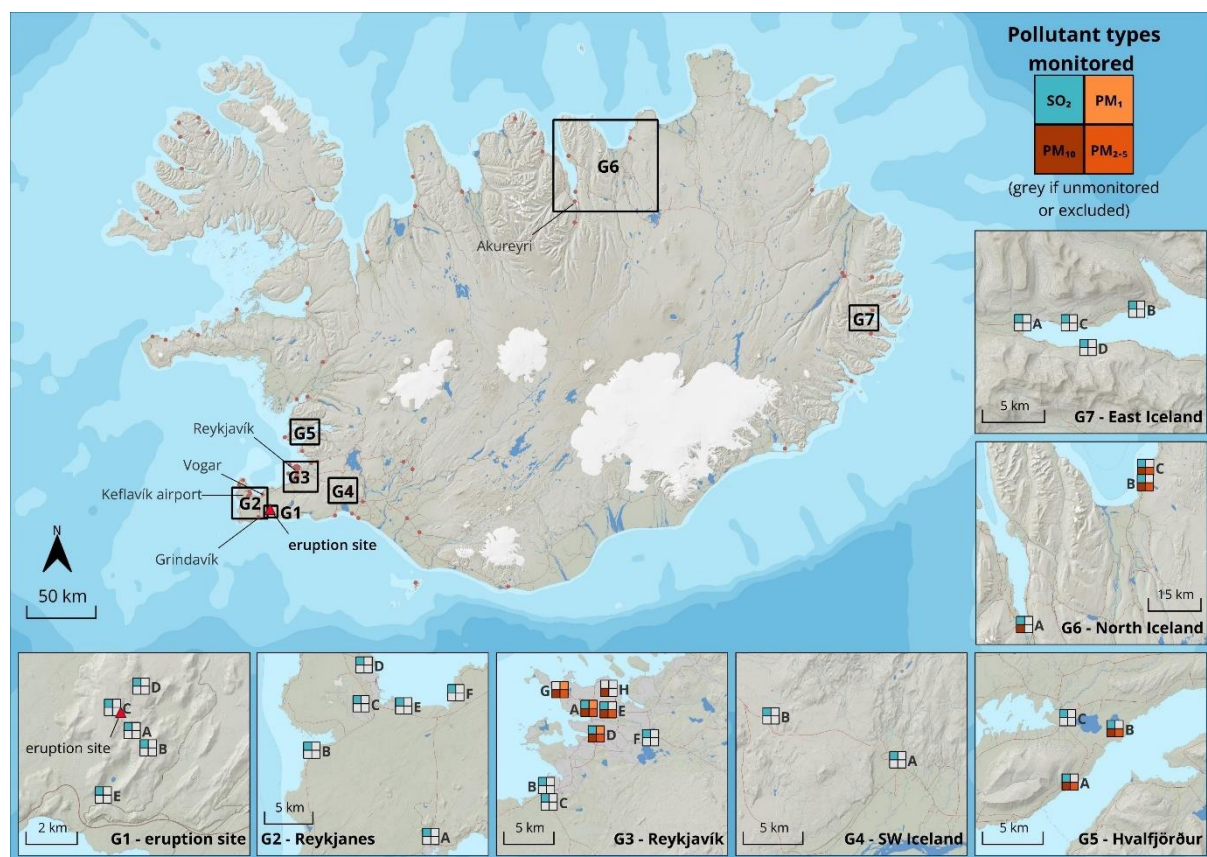


**Figure 1:** Map of Iceland showing the eruption site and air quality monitoring stations. The stations were organised in 7 geographic clusters (each shown on the enlarged inserts). G1 - Eruption site (0-4 km distance from the volcanic vent). G2 - Reykjanes peninsula (9-20 km distance). G3 - Reykjavík capital area (25-35 km distance). G4 - Southwest Iceland (45-55 km distance). G5 - Hvalfjörður (50-55 km distance). G6 - North Iceland (A and B ~280 km, C and D ~330 km distance). G7 - East Iceland (~400 km). The map shows the air pollutant species monitored at each station (SO<sub>2</sub>, PM<sub>10</sub>, PM<sub>2.5</sub>, PM<sub>1</sub>). Areas G2-G7 were monitored with reference-grade stations, while G1 had lower-cost eruption response sensors. Source and copyright of basemap and cartographic elements: Icelandic Met Office & Icelandic Institute of Natural History.



## 110 2 Methods

Measurements were collected by two types of instrument networks: a reference-grade municipal air quality (AQ) network managed by the Environmental Agency of Iceland (EAI, SO<sub>2</sub> and PM in different size fractions); and an eruption-response gas sensor network operated by the Icelandic Meteorological Office (IMO, SO<sub>2</sub> only).

### 2.1 Reference-grade municipal network

115 The EAI network monitors air quality across Iceland according to national legal mandates and complies with Icelandic Directive (ID) regulations. Most of the monitoring stations are in populated areas and measure a variety of air pollutants. Here, we analysed SO<sub>2</sub> and PM in PM<sub>1</sub>, PM<sub>2.5</sub>, PM<sub>10</sub> size fractions, which are the most important volcanic air pollutants with respect to human health in downwind populated areas (Stewart et al., 2021). The detection limits for the majority of the stations in this study were reported to be ~1-3 µg/m<sup>3</sup> SO<sub>2</sub> and < 5 µg/m<sup>3</sup> PM. Station-specific instrument details, detection 120 and resolution limits, and operational duration are in Supplementary Table S1. Figure 1 shows the location of the stations and the air pollutants species measured there.

### 2.2 Eruption site sensors

At the eruption site (0.6-3 km from the active craters), the IMO installed a network of five lower-cost SO<sub>2</sub> sensors between April and July 2021 to monitor air quality in the near-field (specifications and operational length in Table S1). Figure 1 125 shows the location of those eruption-response SO<sub>2</sub> sensors. Stations A, B and E were in close proximity to the public footpaths, while stations C and D were further afield to the north and northwest of the eruption site. The main purpose of the eruption-response network was to alert visitors when SO<sub>2</sub> levels were high rather than to provide accurate SO<sub>2</sub> concentrations. This was because lower-cost air quality sensors (gas and PM) are known to be significantly less accurate than reference-grade instruments (Crilley et al., 2018; Whitty et al., 2022, 2020). Whitty et al., 2022 assessed the 130 performance of lower-cost SO<sub>2</sub> sensors specifically in volcanic environments (same or comparable sensor models to the eruption site stations here) and found that they were frequently subject to interferences restricting their capability to monitor SO<sub>2</sub> in low concentrations. The sensor accuracy limits during field deployment of (Whitty et al., 2022) were significantly poorer than the detection limits reported by the manufacturer. The sensors used in this study were not calibrated or co-located with higher-grade instruments during the field deployment, which seriously limits the accuracy of the obtained data. 135 Due to the low accuracy of the eruption site sensors, especially at lower concentration levels, we analysed the SO<sub>2</sub> data not quantitatively but as yes/no for exceeding the hourly-mean ID air quality threshold of 350 µg/m<sup>3</sup>.

### 2.3 Data processing

SO<sub>2</sub> measurements were downloaded from 24 reference-grade stations and 5 eruption site sensors, and PM<sub>10</sub>, PM<sub>2.5</sub> and PM<sub>1</sub> were downloaded from 12, 11 and 3 reference-grade stations, respectively. Data from reference-grade stations were quality



140 checked and, where needed, re-calibrated by the EAI. Where the operational length was sufficiently long, we obtained  $\text{SO}_2$  and PM measurements for both the eruption period and non-eruptive background period.

We excluded from the analysis reference-grade stations that had data missing for more than 4 months (>70%) of the eruption period. Further details on exclusion reasons of individual stations are in Table S1. This criteria excluded both  $\text{PM}_{10}$  and  $\text{PM}_{2.5}$  from 2 stations (G3-B, G3-C); and  $\text{PM}_{10}$  from one station (G3-H). Data points that were below instrument detection limits 145 were set to 0  $\mu\text{g}/\text{m}^3$  in our analysis. See Table S1 for instrument detection limits of each instrument.

The eruption period was defined as 19/03/2021 20:00 - 19/09/2021 00:00 UTC in agreement with Barsotti et al., 2023. The background period was defined differently for  $\text{SO}_2$  and PM. For  $\text{SO}_2$ , the background period was defined as 19/03/2020 00:00 - 19/03/2021 19:00 UTC, i.e. one full calendar year before the eruption. Outside of volcanic eruption periods,  $\text{SO}_2$  concentrations are generally low with little variability in the Icelandic atmosphere due to an absence of other sources, as 150 shown by previous work (Carlsen et al., 2021a; Ilyinskaya et al., 2017), and subsequently confirmed by this study. The only exception is in the vicinity of aluminium smelters where relatively small pollution episodes occur periodically. A one-year long period was therefore considered as representative of the background  $\text{SO}_2$  fluctuations. We checked our background dataset against a previous comparable in Iceland that used the same methods (Ilyinskaya et al., 2017) and found no statistically-significant difference.

155 PM background concentrations in Iceland are much higher and more variable than  $\text{SO}_2$ . PM frequently reaches high levels in urban and rural areas and there are significant seasonal variations (Carlsen and Thorsteinsson, 2021); the causes of this variability are discussed in the Results and Discussion. To account for this variability, we downloaded PM data for as many non-eruptive years as records existed, and analysed only the period 19 March 20:00 – 19 September 00:00 UTC in each year, i.e. the period corresponding to the calendar dates and months of the 2021 eruption. From here on, we refer to this period as 160 ‘annual period’. The annual periods in 2010, 2011, 2014 and 2015 were partially or entirely excluded from the non-eruptive background analysis due to eruptions in other Icelandic volcanic systems (Eyjafjallajökull 2010, Grímsvötn 2011, Holuhraun 2014-2015) and associated post-eruptive emissions and/or ash resuspension. The annual period of 2022, i.e. the year following the 2021 eruption, was partially included in the background analysis: measurements between 19 March 2022 and 1 August 2022 were included, but measurements from 2 August 2022 were excluded because another eruptive episode started 165 in Fagradalsfjall volcanic system on that date. Since August 2022 there have been 8 more eruptions in the same area at intervals of weeks-to-months, and therefore we have not included more recent non-eruptive background data. Although the 2022 annual period is only partially complete, it was particularly important for statistical analysis of  $\text{PM}_1$  because operational measurements of this pollutant began only in 2020. The number of available background annual periods for  $\text{PM}_{10}$  and  $\text{PM}_{2.5}$  varied depending on when each station was set up, between 1 and 12 stations with an average of 6 (Table S1).

170 We considered whether the year 2020 had lower PM and PM concentrations compared to other non-eruptive years because of COVID-19 pandemic societal restrictions and the extent to which this was likely to impact our results. The societal restrictions in Iceland were relatively light, for example, schools and nurseries remained opened throughout. We found that the average 2020  $\text{PM}_{10}$  and  $\text{PM}_{2.5}$  concentrations fell within the max-min range of the pre-pandemic years for all stations



except at G3-E where  $PM_{10}$  was 10% lower than minimum pre-pandemic annual average, and  $PM_{2.5}$  was 12% lower; and at 175 G5-A where  $PM_{2.5}$  was 25% lower (no difference in  $PM_{10}$ ). G3-E is at a major traffic junction in central Reykjavík, and G5-A is on a major commuter route to the capital area. For  $PM_1$ , only 1 station was already operational in 2020 (G3-A);  $PM_1$  concentrations at this station were 20% higher in 2020 compared to 2022 (post-pandemic). We concluded that PM data from 2020 should be included in our analysis but we do point out the potential impact of pandemic restrictions in the discussion where applicable.

180 **2.4 Data analysis**

We organised the air quality stations into geographic clusters to assess air quality by region. The geographic clusters are the immediate vicinity of the eruption site (G1, 0-4 km distance from the eruption site), the Reykjanes peninsula (G2, 9-20 km distance), the capital area of Reykjavík (G3, 25-35 km distance), Southwest Iceland (G4, 45-55 km distance), Hvalfjörður (G5, 50-55 km distance), North Iceland (G6-A ~280 km, G6-B and C ~330 km distances), and East Iceland (G7, ~400 km 185 distance)(Fig. 1). Appendix B Figs. B1-B7 show  $SO_2$  time series data for each individual station in geographic clusters G1-G7, respectively. Appendix B Figs. B8, B9, B10 show PM time series data for each individual station in geographic clusters G3, G5 and G6, respectively.

For each station that had data for both the eruption and background periods ( $SO_2$  and PM), two-sample t-tests were applied to test whether the background and eruption averages were statistically significantly different for the different pollutant 190 species.

We then calculated the number of events where pollutant concentrations exceeded current air quality thresholds and guidelines. For  $SO_2$ , we used the ID hourly-mean threshold of 350  $\mu g/m^3$  used by the (Icelandic Directive, 2016). For  $PM_{10}$  we used the ID / World Health Organisation (WHO) daily-mean threshold of 50  $\mu g/m^3$ (Icelandic Directive, 2016), and for  $PM_{2.5}$  we used the WHO daily-mean threshold of 15  $\mu g/m^3$ (World Health Organization, 2021), as no ID threshold is defined. 195 There are currently no evidence-based air quality thresholds available for  $PM_1$ . However, the Environmental Agency of Iceland uses a ‘yellow’ threshold for  $PM_1$  at 13  $\mu g/m^3$  when visualising data from the reference-grade stations and this value was used here (‘EAI threshold’).

To be able to meaningfully compare the frequency of air quality threshold exceedance events for  $PM_{10}$ ,  $PM_{2.5}$  and  $PM_1$  (50, 15 and 13  $\mu g/m^3$ , respectively) between the eruption and the non-eruptive background periods we normalised the number of 200 exceedance events, as explained below. This was done because the eruption covered only one annual period (see the definition of ‘annual period’ in 2.3) but the number of available background annual periods varied between stations depending on how long they have been operational, ranging between 1 and 12 periods. We normalised by dividing the total number of exceedance events at a given station by the number of annual periods at the same station. For example, for a station where the non-eruptive background was 6 annual periods the total number of exceedance events was divided by 6 to 205 give a normalised annual number of exceedance events. The eruption covered one annual period and therefore did not require dividing. We refer to this as ‘normalised number of exceedance events’ in the Results and Discussion. Table S1



contains summary statistics for all analysed pollutant means, maximum concentrations, number of air quality threshold exceedances, and number of background annual periods for PM data.

Three reference-grade stations within geographic cluster G3 (Reykjavík capital area) measured all three PM size fractions 210 (PM<sub>1</sub>, PM<sub>2.5</sub> and PM<sub>10</sub>), which allowed us to calculate the relative contribution of different size fractions to the total PM concentration. Since PM size fractions are cumulative, in that PM<sub>10</sub> contains all particles with diameters below  $\leq 10 \mu\text{m}$ , the size modes were subtracted from one another to determine the relative concentrations of particles in the following categories: particles  $\leq 1 \mu\text{m}$  in diameter, 1 - 2.5  $\mu\text{m}$  in diameter and 2.5 - 10  $\mu\text{m}$  in diameter. The comparison of size fractions between the eruption and the background was limited by the relatively short PM<sub>1</sub> timeseries and our results should be re-examined in 215 the future when more non-eruptive measurements have been obtained.

### 3 Results and discussion

#### 3.1 Eruption-driven increase in PM<sub>1</sub> concentrations relative to PM<sub>10</sub> and PM<sub>2.5</sub>

Timeseries of PM<sub>1</sub>, PM<sub>2.5</sub> and PM<sub>10</sub> concentrations were collected at 3 stations in Reykjavík capital (G3-A, G3-D and G3-G, Fig. 1), allowing us to compare the relative contributions of the three size fractions in this area (25-35 km distance from the 220 eruption site). There was a measurable change during the eruption period compared to the background, with an increase in PM<sub>1</sub> mass proportion relative to PM<sub>10</sub> and PM<sub>2.5</sub> at all 3 stations (Fig. 2). The proportion of PM<sub>1</sub> mass within PM<sub>10</sub> increased from 14% in the background to 21-24% during the eruption; and from 23-44% background to 52-57% during the eruption period within PM<sub>2.5</sub>. The change in proportion of PM<sub>2.5</sub> within PM<sub>10</sub> was not as clear, and varied considerably between the 225 stations. Two stations recorded a modest increase in PM<sub>2.5</sub> relative to PM<sub>10</sub>, from 32% background to 37-42% during the eruption period, but the third station recorded a decrease from 60% to 44%.

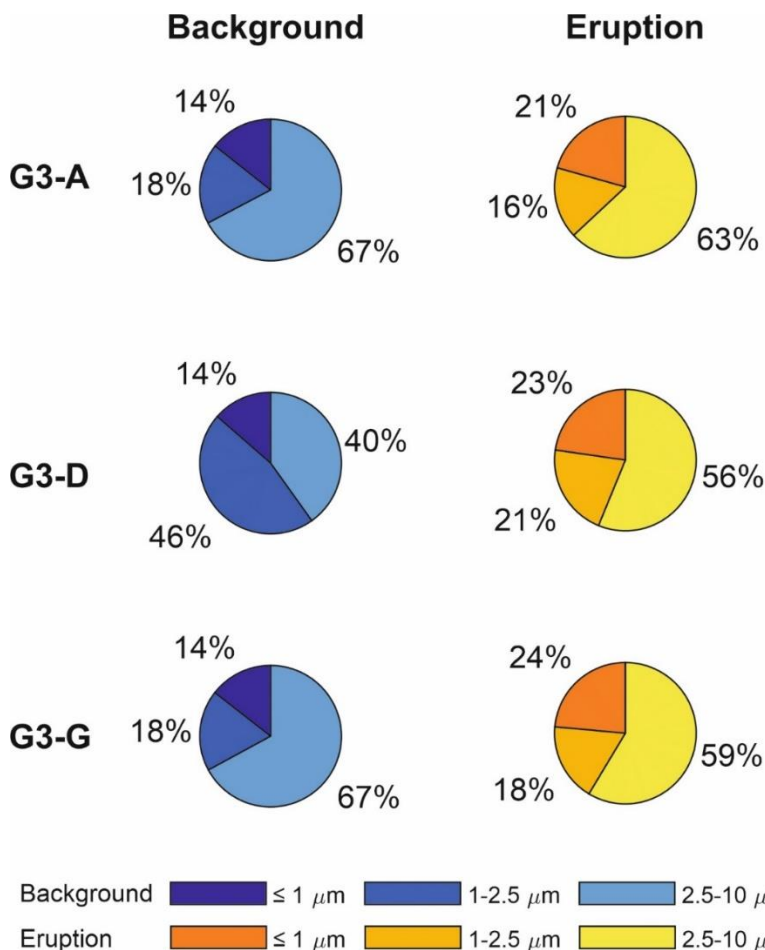


**Figure 2: Relative contribution (in mass%) of three PM size fractions within PM<sub>10</sub> during the non-eruptive background and during the eruption: PM  $\leq 1 \mu\text{m}$  in diameter, PM 1 - 2.5  $\mu\text{m}$  in diameter and PM 2.5 - 10  $\mu\text{m}$  in diameter. G3-A, G3-D and G3-E were the 3 stations in Iceland where all 3 size fractions were measured (all within Reykjavík capital area)**

230 This is a novel result showing that volcanic plumes contribute a significantly higher proportion of PM<sub>1</sub> relative to both PM<sub>10</sub> and PM<sub>2.5</sub> when sampled distally from the source (25-35 km in this study). When sampled at the active vent, volcanic plumes from basaltic fissure eruptions have previously been shown to contain a large amount of PM<sub>1</sub>, but also a substantial proportion of coarse PM ( $> 2.5 \mu\text{m}$ ) (Ilyinskaya et al., 2017; Martin et al., 2011; Mason et al., 2021). At-vent, the composition of the fine and coarse size modes is typically very different, with the finer fraction formed via the conversion of 235 SO<sub>2</sub> gas into sulphate particles, and the coarser fraction made of fragmented silicate material (i.e. ash, which is found in some small concentrations even in typically ash-poor eruptions) (Ilyinskaya et al., 2021). The conversion of SO<sub>2</sub> gas to sulphate particles continues for hours and days after emission from the volcanic vents forming new quantities of fine particles (Green et al., 2019; Pattantyus et al., 2018), while ash particles are not renewed in the plume after emission and are progressively lost through deposition. This can explain the elevated concentrations of particles in the finer size fractions 240 observed downwind of the eruption site relative to the other size fractions. This finding has an implication for the health



hazards posed by volcanic plumes in populated areas, which are typically located at a distance of tens-hundreds of kilometers from the eruption site.

### 3.2 Significant but small increases in average pollutant levels

Most areas of Iceland, up to 400 km distance from the eruption site, recorded a small but statistically significant increase in 245 average  $\text{SO}_2$  and PM concentrations during the eruption compared to the background period.

Figure 3 and Table 1 compare  $\text{SO}_2$  concentrations (hourly-means,  $\mu\text{g}/\text{m}^3$ ), measured by reference-grade stations across Iceland. During the non-eruptive background period,  $\text{SO}_2$  concentrations were low (long term hourly-mean average generally <2  $\mu\text{g}/\text{m}^3$ ), which is in agreement with previous studies (Ilyinskaya et al., 2017). Stations in the vicinity of aluminium smelters (G5-1 and 2, G6-C and G7-all) had higher long-term average values and periodically measured short-lived 250 escalations in  $\text{SO}_2$  hourly-mean concentrations of several 10s or 100s of  $\mu\text{g}/\text{m}^3$  during the background period (Fig. 3, Table 1 and Table S1). Station G7-D (East Iceland at ~400 km distance from the eruption site) was the only one where the eruption-related increase in average  $\text{SO}_2$  concentrations was below statistical significance. This station was in a vicinity of an aluminium smelter, and was also missing over 1/3 of the eruption period data due to technical issues, which may have reduced the observed eruption impact.

255 The average  $\text{SO}_2$  concentrations were higher during the eruption at all reference-grade stations that had data from both before and during the eruption ( $n=16$ ), and the increase was statistically significant ( $p<0.05$ ) at 15 out of the 16 stations. Across all 7 geographic clusters, the absolute increase in average  $\text{SO}_2$  concentrations between the background and eruption period was relatively low, on the order of a few  $\mu\text{g}/\text{m}^3$  (Fig. 3 and Table 1). For example, the average concentration across Reykjavík capital changed from 0.32  $\mu\text{g}/\text{m}^3$  in the background to 4.1  $\mu\text{g}/\text{m}^3$  during eruption.

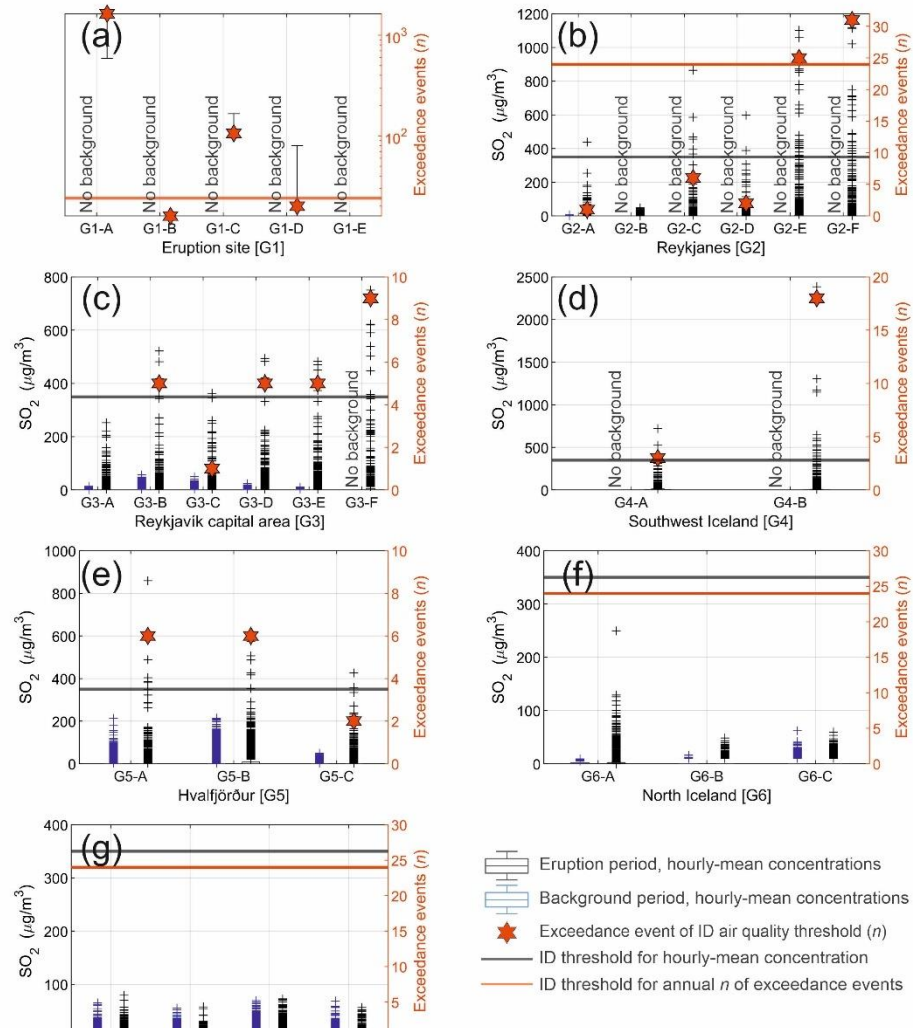
260 The absolute increases in average PM concentrations in all measured size fractions were relatively modest, similar to the change observed in  $\text{SO}_2$  average concentrations. Table 2 and Figs. 4-6 show  $\text{PM}_{10}$ ,  $\text{PM}_{2.5}$  and  $\text{PM}_1$  concentrations (daily-means,  $\mu\text{g}/\text{m}^3$ ) measured in the 3 geographic area where reference-grade monitoring was available. For example, in Reykjavík capital (at stations where concentrations during the eruption period were statistically-significantly higher than background), the average  $\text{PM}_{10}$  concentration changed from 9-10  $\mu\text{g}/\text{m}^3$  in the background to 12-13  $\mu\text{g}/\text{m}^3$  during the 265 eruption period; average  $\text{PM}_{2.5}$  from 3-4  $\mu\text{g}/\text{m}^3$  background to ~5  $\mu\text{g}/\text{m}^3$  eruption; and average  $\text{PM}_1$  from 1.3-1.5  $\mu\text{g}/\text{m}^3$  background to ~3  $\mu\text{g}/\text{m}^3$  eruption (Fig. 4).

270 **Table 1:  $\text{SO}_2$  concentrations (hourly-mean,  $\mu\text{g}/\text{m}^3$ ) in populated areas around Iceland during the non-eruptive background and during the Fagradalsfjall 2021 eruption. ‘Average’ is the average hourly-mean of all stations within a geographic area. ‘Peak’ is the maximum hourly-mean recorded by an individual station within the geographic area. ‘ID exceedances’: number of times that the  $\text{SO}_2$  concentrations exceeded the Icelandic Directive air quality threshold of 350  $\mu\text{g}/\text{m}^3$ . Number of AQ exceedances is the maximum number of exceedances recorded by an individual station within a geographic area.**

Geographic	N of	Distance	$\text{SO}_2$ hourly-mean ( $\mu\text{g}/\text{m}^3$ )				ID exceedances (max n)	
			Background	Eruption	Background	Eruption	Background	Eruption

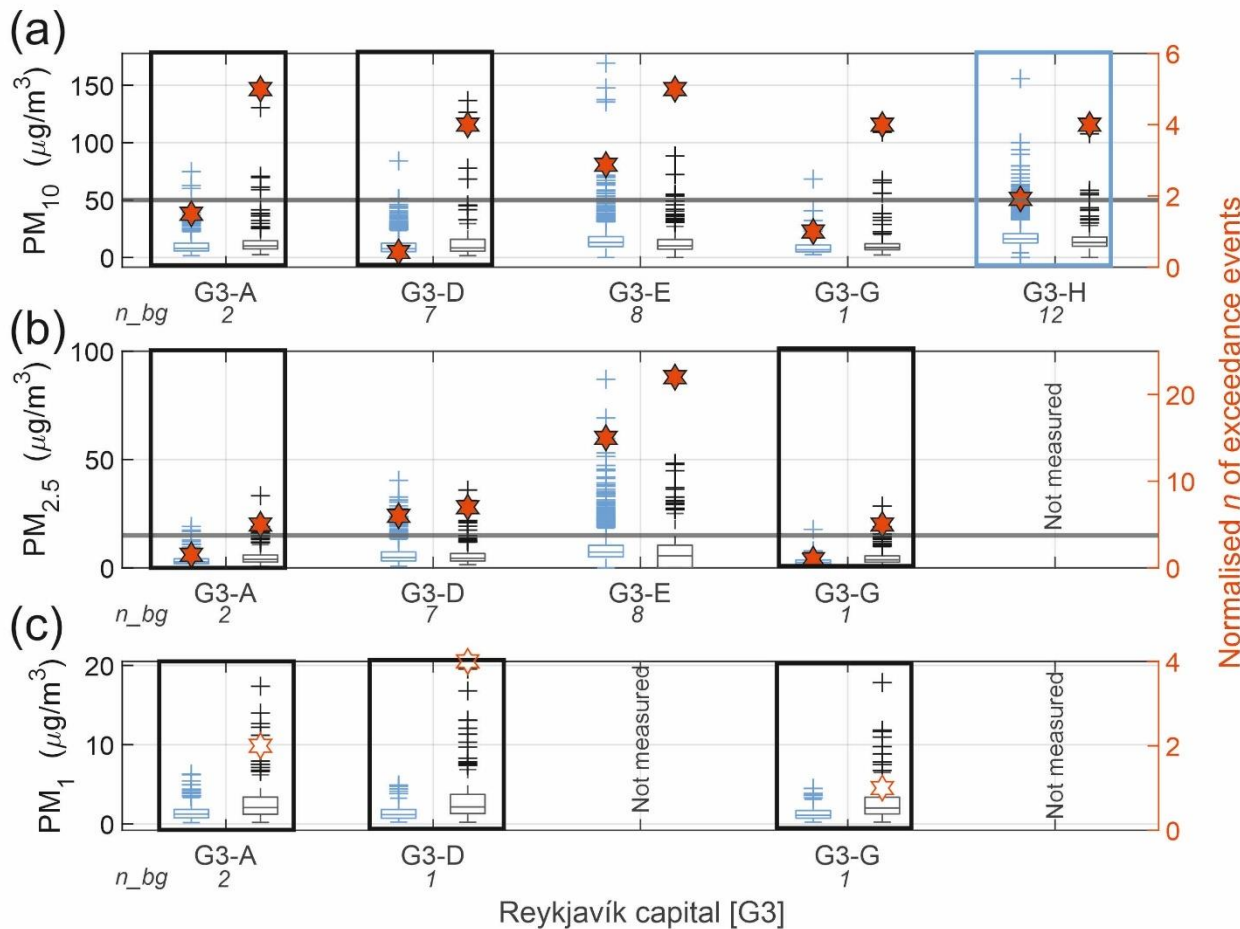


area	stations	from eruption site (km)	average	average	peak	peak		
Reykjanes peninsula (G2)	6	9-20	0.14	4.6	7.7	2400	0	31
Reykjavík capital (G3)	6	25-35	0.32	4.1	57	750	0	9
South Iceland (G4)	2	45-55	No data	6.1	No data	2400	No data	18
Hvalfjörður (G5)	3	50-55	3.8	8.2	210	860	0	6
North Iceland (G6)	3	280-330	0.38	1.7	9.1 at 280 km; 62 at 330 km	250 at 280 km; 48 at 330 km	0	0
East Iceland (G7)	4	400	1.8	2.4	69	79	0	0



275 **Figure 3: Hourly-mean concentrations and number of ID threshold exceedance events for  $\text{SO}_2$  ( $\mu\text{g}/\text{m}^3$ ), measured by 29 stations across 7 geographical areas in Iceland (a-g). The data are shown as box-and-whiskers plots, with crosses representing extremely high values (statistical outliers). Pre-eruptive background is shown for stations that were in operation before the eruption started. Panel (a) shows eruption-site measurements collected by lower-accuracy sensors for which we only report number of exceedances of the ID air quality threshold ( $350 \mu\text{g}/\text{m}^3$ ). Panels (b-g) show data from reference-grade stations in populated areas as  $\text{SO}_2$  hourly-mean concentrations and the number of exceedance events. The ID air quality threshold of  $350 \mu\text{g}/\text{m}^3$  hourly-mean is shown on all panels with a black horizontal line. The figure also shows whether the number of threshold exceedances at each station exceeded the recommended annual total ( $n=24$ , orange horizontal line). Note logarithmic scale for Eruption site (a). Time series plots for each station are available in Appendix B Figures B1-B7.**

280



- Eruption period, daily-mean concentration
- Background period, daily-mean concentration
- Eruption-mean significantly higher than background-mean
- Background-mean significantly higher than eruption-mean
- $n_{bg}$  Number of analysed background periods
- ★ Normalised  $n$  of exceedance events
- ID / WHO threshold for daily-mean concentration

285 **Figure 4: Daily-mean concentrations of (a) PM<sub>10</sub>, (b) PM<sub>2.5</sub> and (c) PM<sub>1</sub> ( $\mu\text{g}/\text{m}^3$ ), measured in Reykjavík capital area.** The concentrations are shown as box-and-whiskers plots, with crosses representing extremely high values (statistical outliers). Pre-eruptive background is shown for stations which were in operation before the eruption started,  $n_{bg}$  indicates the number of background annual periods for each station (see Methods for definition of a background annual period). Stations where the average concentration during the eruption period was statistically-significantly higher than the background are highlighted with a black box. Stations where the average concentration during the eruption period was statistically-significantly lower than the background are highlighted with a blue box. Absence of a box indicates no significant difference between eruption and background periods. The figure shows the normalised number of times PM<sub>10</sub> and PM<sub>2.5</sub> concentrations at each station exceeded the ID air quality threshold of 50 and 15  $\mu\text{g}/\text{m}^3$  daily-mean, respectively. For PM<sub>1</sub>, the figure shows the number of times the concentration during the eruption exceeded the EAI threshold of 13  $\mu\text{g}/\text{m}^3$  daily-mean. The number of threshold exceedance events is normalised to the length of the measurement period – refer to the main text for an explanation of the method. Time series plots for each station are available in Appendix B Figure B8.

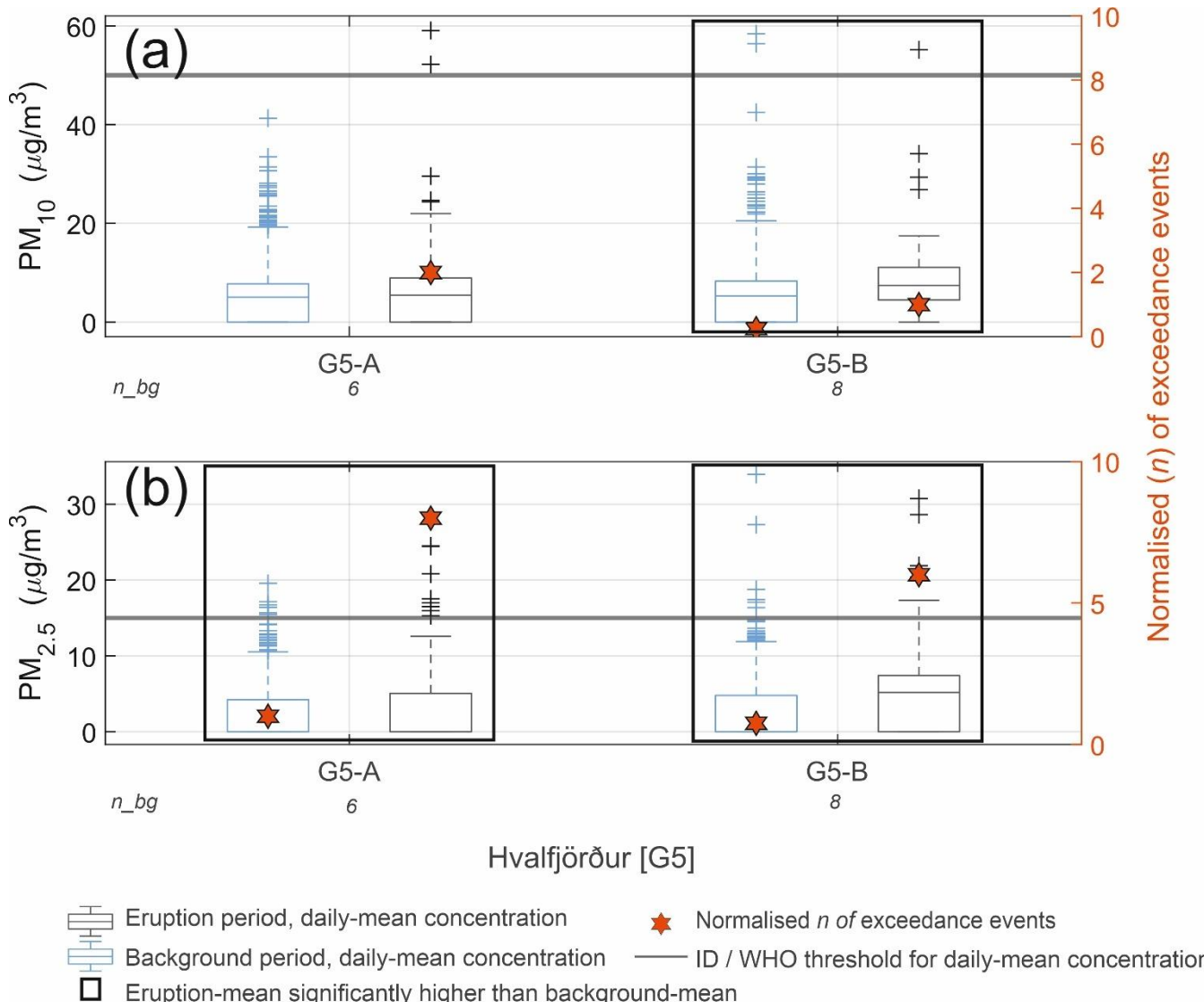
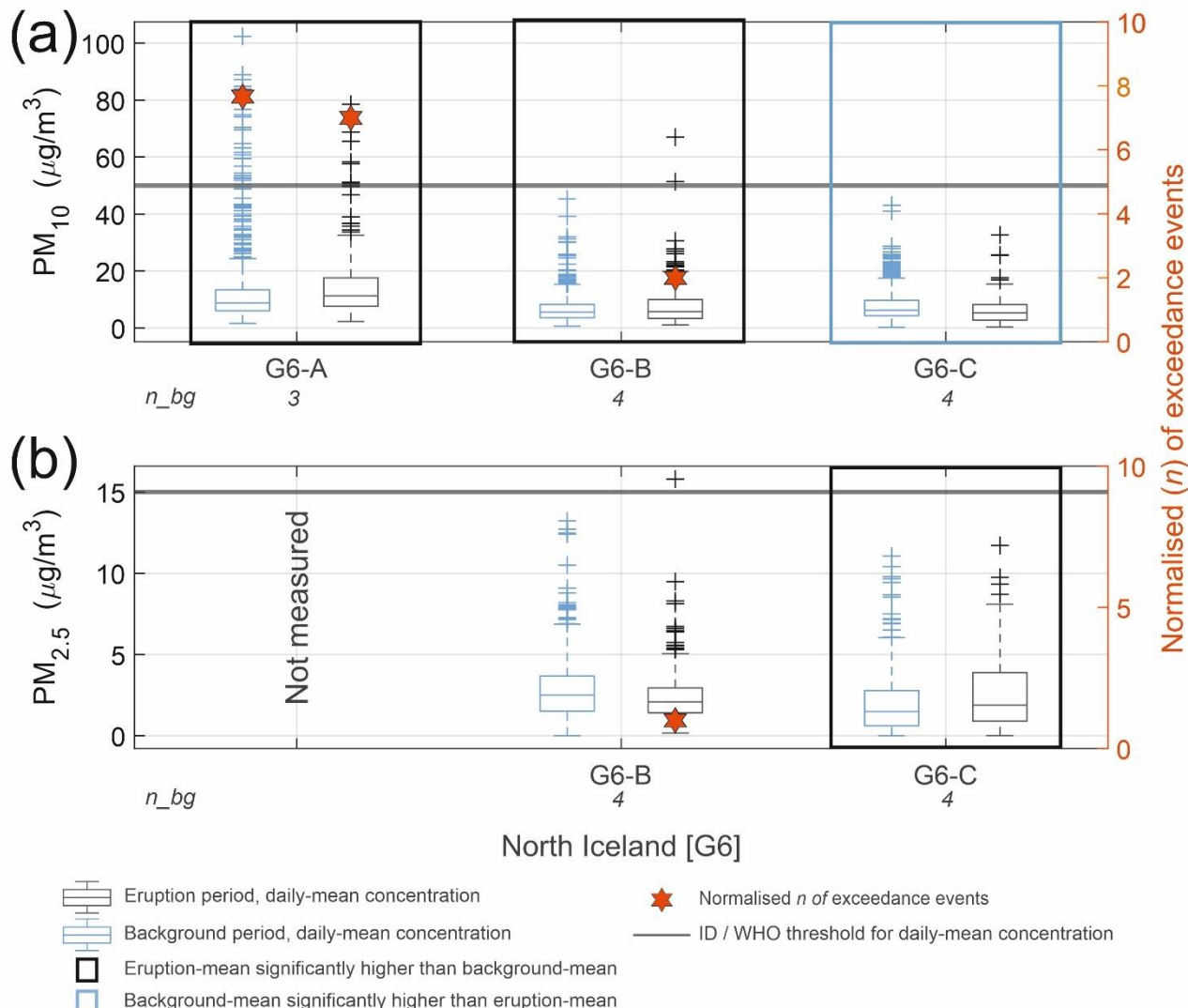


Figure 5: Daily-mean concentrations of (a)  $\text{PM}_{10}$ , and (b)  $\text{PM}_{2.5}$  ( $\mu\text{g}/\text{m}^3$ ), measured in Hvalfjörður area. The concentrations are shown as box-and-whiskers plots, with crosses representing extremely high values (statistical outliers). Pre-eruptive background is shown for stations which were in operation before the eruption started,  $n_{bg}$  indicates the number of background annual periods for each station (see methods for definition of a background annual period). Stations where the average concentration during the eruption period was statistically-significantly higher than the background are highlighted with a black box (absence of a box indicates no significant difference). The figure shows the normalised number of times  $\text{PM}_{10}$  and  $\text{PM}_{2.5}$  concentrations at each station exceeded the ID air quality threshold of 50 and 15  $\mu\text{g}/\text{m}^3$  daily-mean, respectively. The number of threshold exceedance events is normalised to the length of the measurement period – refer to the main text for an explanation of the method. Time series plots for each station are available in Appendix B Figure B9.



**Figure 6: Daily-mean concentrations of (a) PM<sub>10</sub>, and (b) PM<sub>2.5</sub> ( $\mu\text{g}/\text{m}^3$ ), measured in North Iceland. The concentrations are shown as box-and-whiskers plots, with crosses representing extremely high values (statistical outliers). Pre-eruptive background is shown for stations which were in operation before the eruption started,  $n_{bg}$  indicates the number of background annual periods for each station (see methods for definition of a background annual period). Stations where the average concentration during the eruption period was statistically-significantly lower than the background are highlighted with a blue box. Absence of a box indicates no significant difference between eruption and background. The figure shows the normalised number of times PM<sub>10</sub> and PM<sub>2.5</sub> concentrations at each station exceeded the ID air quality threshold of 50 and 15  $\mu\text{g}/\text{m}^3$  daily-mean, respectively. The number of threshold exceedance events is normalised to the length of the measurement period – refer to the main text for an explanation of the method. Time series plots for each station are available in Appendix B Figure B10.**

310

315



320 **Table 2 PM<sub>10</sub>, PM<sub>2.5</sub> and PM<sub>1</sub> concentrations (µg/m<sup>3</sup>, 24-h mean) in populated areas around Iceland during the non-eruptive background ('b/g') and during the Fagradalsfjall 2021 eruption ('erupt.'). 'Average' is the average 24 h-mean of all stations within the geographic area. 'Peak' is the maximum 24 h-mean recorded by an individual station within a geographic area. 'AQ exceedances' is number of times that the PM concentrations exceeded the following concentrations: PM<sub>10</sub> 50 µg/m<sup>3</sup> 24 h-mean; PM<sub>2.5</sub> 15 µg/m<sup>3</sup> 24 h-mean; PM<sub>1</sub> 13 µg/m<sup>3</sup> 24h-mean. 'AQ exceedances' is the maximum number of exceedances recorded by an individual station within a geographic area.**

Geographic area	n of stations (PM10, PM2.5, PM1)	Distance from eruption site (km)	PM <sub>10</sub>				PM <sub>2.5</sub>				PM <sub>1</sub>									
			Average (µg/m <sup>3</sup> , 24-h mean)		Peak (µg/m <sup>3</sup> , 24-h mean)		AQ exceedances (max n)		Average (µg/m <sup>3</sup> )		Peak (µg/m <sup>3</sup> , 24-h mean)		AQ exceedances (max n)		Average (µg/m <sup>3</sup> , 24-h mean)		Peak (µg/m <sup>3</sup> , 24-h mean)		AQ exceedances (max n)	
			B/G	Erup t.	B/G	Erup t.	B/G	Erup t.	B/G	Erup t.	B/G	Erup t.	B/G	Erup t.	B/G	Erup t.	B/G	Erup t.		
Reykjavík capital (G3)	5, 4, 3	25-35	11	13	170	140	2.9	5	4.6	5.3	87	48	15	22	1.4	2.8	6.3	20	0	4
Hvalfjörður (G5)	3	50-55	5.7	7.6	58	59	0.25	2	2.1	4.2	34	31	1	8	No data					
North Iceland (G6)	3	280-330	8.1	8.6	100	79	7.7	7	0.53	0.72	13	16	0	1						



Generally,  $PM_{1}$  and  $PM_{2.5}$  showed a more consistent eruption-related increase than  $PM_{10}$ , which agrees with our results on their relative proportions discussed in 3.1. During the eruption,  $PM_{1}$  average concentrations were statistically-significantly higher at all monitored stations in Reykjavík capital (G3, Fig. 4). The  $PM_{2.5}$  and  $PM_{10}$  concentrations were statistically-significantly higher during the eruption at approximately half of the monitored stations across all geographic stations (Figs. 330 4-6). The locations that recorded significant eruption-related increases in average  $PM_{10}$  and  $PM_{2.5}$  concentrations generally had lower non-eruptive background concentrations. The stations with higher background  $PM_{10}$  and  $PM_{2.5}$  were generally located closer to roads with heavy traffic; this shows that local sources such as road traffic were more important  $PM_{10}$  and 335  $PM_{2.5}$  pollution sources than the distal eruption, but the eruption impacts on average levels of  $PM_{10}$  and  $PM_{2.5}$  were more noticeable in areas with lower background concentrations. Average levels of  $PM_{1}$  were unequivocally higher during the eruption period compared to the background, but this pollutant was only monitored in the Reykjavík capital area. It remains to be investigated whether volcanic contribution to  $PM_{1}$  would also dominate over other sources in more distal communities.

### 3.3 Impact on pollutant peak concentrations and number of air quality exceedance events

Unlike the modest (or, at some stations, negligible) increases in the average concentrations of PM and  $SO_2$ , the eruption was 340 associated with large increases in the number of air quality threshold exceedance events in the near- and far-field.

Figure 3 and Table 1 compare the background and the eruption periods with respect to peak concentrations, and the number of Iceland Directive (ID) threshold exceedance events for  $SO_2$  ( $350 \mu g/m^3$  hourly-mean). During the non-eruptive background the  $SO_2$  concentrations never exceeded the ID threshold at any of the stations. During the eruption, the numbers of threshold exceedance events ranged between 0 and 31 at individual stations and were, broadly speaking, the highest closer 345 to the eruption site (Fig. 3 and Table 1). However, there were noticeable fine-scale spatial variations in  $SO_2$  concentrations within individual geographical areas as discussed further in 3.4. The ID threshold for total annual hourly-mean exceedances ( $n=24$ ) was exceeded in the geographic cluster in the immediate vicinity of the eruption site (G1; up to 1600 events at an individual station), and in two communities on the Reykjanes peninsula (G2; 25 and 31 events, respectively). We attributed the combination of a relatively low absolute increase in the average  $SO_2$  concentrations, and a large increase in peak 350 concentrations to a combination of the pulsating behaviour of the eruption emissions, and highly variable local meteorological conditions (wind rose for eruption site is in Appendix B Fig. B11 (Barsotti et al., 2023; Pfeffer et al., 2024)). This meant that the volcanic plume was only periodically advected into individual populated areas, rather than being a persistent source of pollution in the same location.

$PM_{1}$  concentrations never exceeded the EAI threshold ( $13 \mu g/m^3$ ) in the background period but during the eruption exceeded 355 between 3 and 5 times at all stations where it was monitored (Fig. 4, Table 2). The number of  $PM_{10}$  and  $PM_{2.5}$  exceedance events was higher during the eruption period at all stations in Reykjavík capital area (G3) and in Hvalfjörður (G5), and at 2 out of 3 North Iceland (G6) stations that recorded any threshold exceedances.

$PM_{1}$  peak concentrations increased from  $5-6 \mu g/m^3$  peak daily-mean during the background period to  $\sim 20 \mu g/m^3$  peak daily-mean during the eruption period, across all 3 monitored stations in Reykjavík capital (G3). Volcanic impact on  $PM_{10}$  and



360 PM<sub>2.5</sub> was more variable compared to PM<sub>1</sub>. Reykjavík capital stations with cleaner PM<sub>10</sub> and PM<sub>2.5</sub> backgrounds (peak daily-mean <80 µg/m<sup>3</sup> PM<sub>10</sub> and <20 µg/m<sup>3</sup> PM<sub>2.5</sub>) showed larger impacts from the eruption than stations with more polluted background conditions (peak daily-means  $\geq$ 110 µg/m<sup>3</sup> PM<sub>10</sub> and  $\geq$ 40 µg/m<sup>3</sup> PM<sub>2.5</sub>). The cleaner stations show eruption-related increases of up to 40-60 µg/m<sup>3</sup> PM<sub>10</sub> and 10-14 µg/m<sup>3</sup> PM<sub>2.5</sub> above peak background levels while the more polluted stations did not have noticeable increases in peak daily-means of PM<sub>10</sub> and PM<sub>2.5</sub> during the eruption. Further afield, in  
365 Hvalfjörður and North Iceland (Figs. 5-6), the number of monitoring stations was too low for a statistical analysis, but generally the same pattern was observed: stations with lower non-eruptive background PM<sub>10</sub> and PM<sub>2.5</sub> generally recorded increases in peak daily-mean concentrations of up to  $\sim$ 20 and 5 µg/m<sup>3</sup>, respectively, above background levels.  
The statistically significant impact on average and peak PM levels observed in the Reykjavík capital and further afield (in up to at least 300 km distance) is remarkable considering the relatively small size of the eruption and the importance of non-  
370 volcanic PM sources in Iceland. In rural areas, the main non-volcanic source of PM is re-suspended natural dust sourced from highland deserts (Butwin et al., 2019), with higher levels in the drier summer seasons. In urban areas, the non-volcanic PM pollution peaks are typically higher in the winter with the main source being tarmac road erosion by studded tyres (Carlsen and Thorsteinsson, 2021). The unequivocal eruption-related increase in average and peak concentrations of PM<sub>1</sub> suggests that volcanic fissure eruptions are one of, or potentially the most, important source of PM<sub>1</sub> in Iceland, at least during  
375 the summer months. Table 3 compares concentration ratios of the three measured PM size fractions in Reykjavík between a representative eruption-free background; the 2021 volcanic plume; and two Icelandic desert dust storms in 2023. The comparison is made based on a small dataset but suggests distinct ‘fingerprint’ ratios for the different pollution sources. These ratios may be used for identifying sources of PM pollution episodes in Reykjavík and potentially other distal populated areas, especially when the sources are difficult to identify using meteorological and/or visual observations. During  
380 the winter months, the contribution of tarmac erosion by studded tyres may affect the ratios; and higher short-lived peak concentrations may happen during New Years Eve fireworks – more data on winter-time eruptions is needed to establish this.



**Table 3. Concentration ratios of PM size fractions (hourly-means,  $\mu\text{g}/\text{m}^3$ ) associated with different pollution sources in Reykjavík capital area. Green-coloured rows show ratios during periods considered to be representative of typical Reykjavík background: ‘Summer period’ when studded tyres are not in use (banned between 14 April and 31 October), and a period during the 2021 eruption when the plume was being advected away from Reykjavík. Orange-coloured rows show ratios during the 2021 eruption when the plume was advected to Reykjavík; for definitions of fresh and mature plume see section 3.4. ‘Desert dust’ are pollution episodes caused by Icelandic highland desert storms (source area ~200 km from Reykjavík), confirmed by IMO meteorological and visual observations. Station G3-G is listed first as it is considered to be the most sensitive one to the presence of volcanic plume due to low background concentrations from local sources.**

	Start date	Start time	End date	End time	G3-G	G3-A	G3-D	G3-G	G3-A	G3-D	G3-G	G3-A	G3-D
					PM <sub>1</sub> /PM <sub>10</sub>	PM <sub>1</sub> /PM <sub>10</sub>	PM <sub>1</sub> /PM <sub>10</sub>	PM <sub>1</sub> /PM <sub>2.5</sub>	PM <sub>1</sub> /PM <sub>2.5</sub>	PM <sub>1</sub> /PM <sub>2.5</sub>	PM <sub>2.5</sub> /PM <sub>10</sub>	PM <sub>2.5</sub> /PM <sub>10</sub>	PM <sub>2.5</sub> /PM <sub>10</sub>
Summer period, no eruption	01/05/2020	00:00	01/09/2020	00:00	0.16	0.15	0.13	0.44	0.43	0.22	0.35	0.34	0.61
Eruption but no plume in Reykjavík	01/04/2021	09:00	02/04/2021	10:00	0.17	0.19	0.24	0.41	0.43	0.45	0.42	0.43	0.54
Fresh plume	18/07/2021	10:00	19/07/2021	16:00	0.65	0.68	0.7	0.9	0.92	0.84	0.72	0.73	0.78
Mature plume 1	28/04/2021	08:00	29/04/2021	20:00	0.43	0.29	0.49	0.8	0.73	0.8	0.53	0.39	0.6
Mature plume 2	19/05/2021	14:00	21/05/2021	11:00	0.71	0.65	0.85	0.96	0.95	0.95	0.73	0.68	0.89
Mature plume 3	01/07/2021	09:00	06/07/2021	08:00	0.67	0.59	0.65	0.91	0.88	0.84	0.74	0.66	0.74
Desert dust 1	03/11/2023	13:00	04/11/2023	02:00	0.02	n/a	0.02	0.11	n/a	0.13	0.15	n/a	0.15
Desert dust 2	08/11/2023	14:00	09/11/2023	00:00	0.01	n/a	0.01	0.1	n/a	0.086	0.15	n/a	0.15



### 3.4 Fine-scale temporal and spatial variability in SO<sub>2</sub> and PM<sub>1</sub> peaks

395 The dense reference-grade network between 9 and 35 km from the eruption site (clusters G2 and G3) revealed fine-scale variability at these relatively distal sites. Five out of 6 stations on Reykjanes peninsula (SO<sub>2</sub> only) were north and northwest from the eruption site, within the most common wind direction (wind rose in Fig. B11). Despite only 3-16 km distance between these stations, two of them (G2-E and G2-F) recorded 25 and 31 SO<sub>2</sub> hourly-mean exceedance events, respectively, while G2-B, G2-C and G2-D recorded between 0 and 6 events (Fig. 3). To test that this was not an artifact of some of the  
400 stations having been set up later than others during the eruption, we also counted the number of exceedance events from 7 May 2021, the date by which all G2 stations had become operational. The result was largely unchanged: the number of exceedance events remained higher at G2-E and F (7 and 26 events, respectively) and lower at G2-B, C, and D (0-6 events). The spatio-temporal difference between the ‘high exceedance stations’ G2-E and G2-F, which were within 5 km distance of each other is also noteworthy: during the first 7 weeks of the eruption (19 March – 7 May 2021) G2-E recorded 18 of its total  
405 25 exceedance events, while G2-F recorded only 5 out of 31. This likely reflects the control of the wind direction rather than topography as both stations were close to sea level, and demonstrates that the edges of the volcanic pollution cloud were sharply defined.

Reykjavík capital area stations (G3) were located 25-35 km from the eruption site and within <1 and 10 km from one another (Fig. 1). The most significant volcanic plume advection episode happened on 18-19 July 2021, when the G3 stations  
410 cumulatively recorded 21 SO<sub>2</sub> hourly-mean air quality exceedance events out of the 23 recorded during the whole eruption. This advection episode revealed how the concentrations of volcanic pollutants varied on a fine spatio-temporal scale. Figures 7a-7d show the spatio-temporal resolution and ratios of SO<sub>2</sub> and PM as hourly-means during this episode. We focus this discussion on PM<sub>1</sub> rather than PM<sub>2.5</sub> and PM<sub>10</sub> because PM<sub>1</sub> more clearly represented the volcanic source compared to the other size fractions, as discussed in 3.1 and shown on Figs. 7c-7d. Both SO<sub>2</sub> and PM<sub>1</sub> were highly elevated above  
415 background concentrations during the advection episode at all G3 stations (Figs. 7a-7d). Stations G3-A and G3-E were located < 1 km of each other; during the 18-19 July episode G3-E recorded ~2 times higher maximum SO<sub>2</sub> concentrations than G3-A (480 and 250 µg/m<sup>3</sup>, respectively), and five SO<sub>2</sub> air quality threshold exceedance events while G3-A recorded zero (Figs. 2 and 7a). The fine scale spatio-temporal differences were also observed in PM<sub>1</sub>: for example, G3-D recorded up to twice as high PM<sub>1</sub> hourly-means than G3-G during the same advection episode (Fig. 7b). The topographic elevation  
420 difference between G3 stations is unlikely to explain the spatial fluctuations as it is relatively small. Most of the G3 stations are located between 10 and 40 m above sea level (a.s.l.) and G3-F is at 85 m a.s.l.. One potential contributing factor could be channelling and/or downwash of air currents by urban buildings, a process that might be important for central Reykjavík locations, and requires further investigation, e.g. by fine-scale dispersion modelling, but is beyond the scope of this study.  
The relative proportions of the two pollutants, SO<sub>2</sub> and PM<sub>1</sub>, in the 18-19 July advection episode varied strongly between the  
425 two stations that measured both of them (G3-A and G3-D). The SO<sub>2</sub> peak hourly-mean differed by nearly a factor of 2 between the two stations (Fig. 7a); but PM<sub>1</sub> peak hourly-means only by a maximum of 20% (Fig. 7b). During the advection



episode, both pollutants showed 3 principal concentration peaks. The first of the three principal concentration peaks (July 18 13:00) recorded the highest SO<sub>2</sub> concentration at station G3-D, and the last of the 3 pollution peaks (July 19 23:00) recorded the highest PM<sub>1</sub> concentration at the same station (Figs 7a-7b).

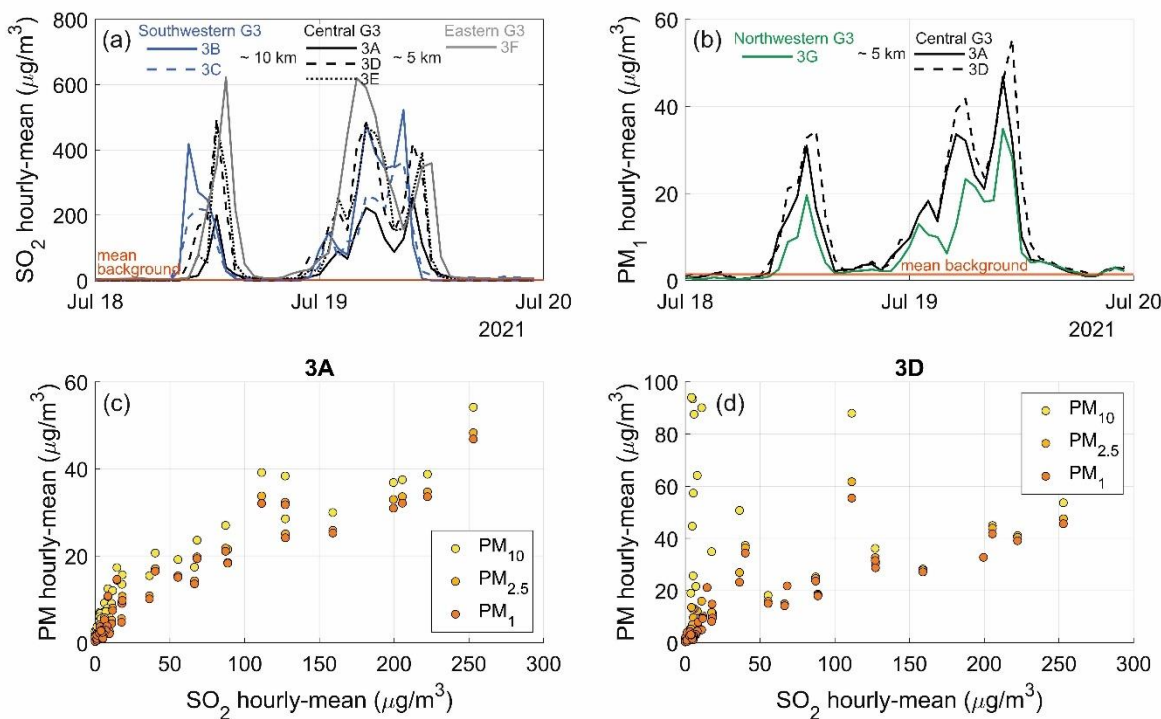


**Figure 7: SO<sub>2</sub> and PM concentrations (µg/m<sup>3</sup>) during a ‘fresh’ volcanic plume advection episode in Reykjavík capital area (G3) 18-19 July 2021. 3A to 3F are names of reference-grade stations and the figure indicates their respective locations within Reykjavík (southwestern, central, eastern, and northwestern) and the approximate distance between them. Panel (a): SO<sub>2</sub> hourly-means timeseries. Panel (b): PM<sub>1</sub> hourly-means timeseries. Panel (c): Scatter plot between concentrations of SO<sub>2</sub> and PM<sub>10</sub>, PM<sub>2.5</sub> and PM<sub>1</sub> at station 3A, which measured all of these pollutants. Panel (d): Scatter plot between concentrations of SO<sub>2</sub> and PM<sub>10</sub>, PM<sub>2.5</sub> and PM<sub>1</sub> at station 3D, which measured all of these pollutants.**

430

435

440

445

We also examined the fluctuations in SO<sub>2</sub> and PM<sub>1</sub> during an advection episode of a chemically mature plume locally known as ‘móða’, or ‘vog’ in English (volcanic smog) in Reykjavík capital area July 1-7 2021 (Fig. 8a-8d). A chemically mature plume has undergone significant gas-to-particle conversion of sulphur in the atmosphere and, as shown by Ilyinskaya et al., 2017, may be advected into the populated area some days after the initial emission. The mature plume (Figs. 8c-8d) has a higher PM/SO<sub>2</sub> ratio than a fresh plume (Figs. 7c-7d), and SO<sub>2</sub> is elevated to above-background levels to a variable degree, sometimes only slightly (Ilyinskaya et al., 2017). Conditions which would typically facilitate the generation of móða and its accumulation are low wind speed, high humidity and intense solar radiation. Based on these factors, the 1-7 July episode was identified by IMO at the time of the event as móða, and a public air quality advisory was issued. Figs. 8c-8d shows that



during the móða event  $\text{PM}_1$  is frequently elevated without a correspondingly-high increase in  $\text{SO}_2$ . The highest peaks of  $\text{SO}_2$  were well-defined but  $\text{PM}_1$  was highly elevated above background levels throughout the whole period with less prominent individual concentration peaks. It is possible that  $\text{PM}_1$  grounds more persistently than  $\text{SO}_2$ , which could be tested in follow-on work by dispersion modelling with high vertical resolution near ground level.

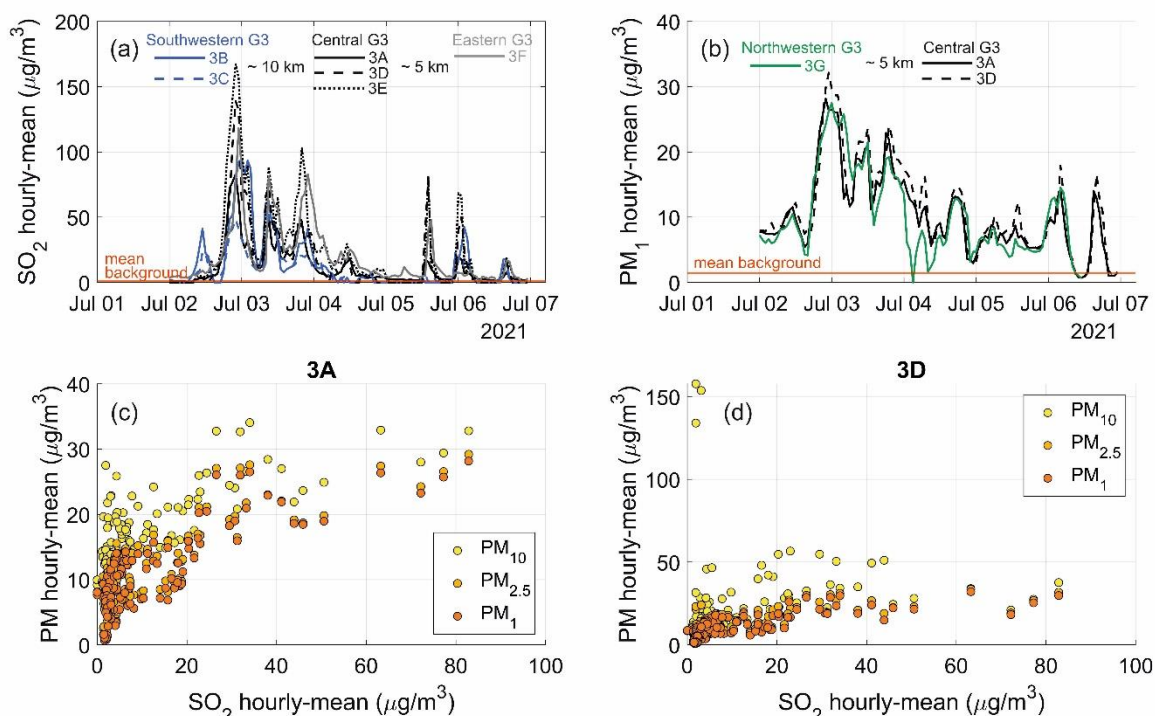


Figure 8:  $\text{SO}_2$  and PM concentrations ( $\mu\text{g}/\text{m}^3$ ) during a ‘mature’ volcanic plume advection episode in Reykjavík capital area (G3) 1-7 July 2021. 3A to 3F are names of reference-grade stations and the figure indicates their respective locations within Reykjavík (southwestern, central, eastern, and northwestern) and the approximate distance between them. Panel (a):  $\text{SO}_2$  hourly-means timeseries. Panel (b):  $\text{PM}_1$  hourly-means timeseries. Panel (c): Scatter plot between concentrations of  $\text{SO}_2$  and  $\text{PM}_{10}$ ,  $\text{PM}_{2.5}$  and  $\text{PM}_1$  at station 3A, which measured all of these pollutants. Panel (d): Scatter plot between concentrations of  $\text{SO}_2$  and  $\text{PM}_{10}$ ,  $\text{PM}_{2.5}$  and  $\text{PM}_1$  at station 3D, which measured all of these pollutants.

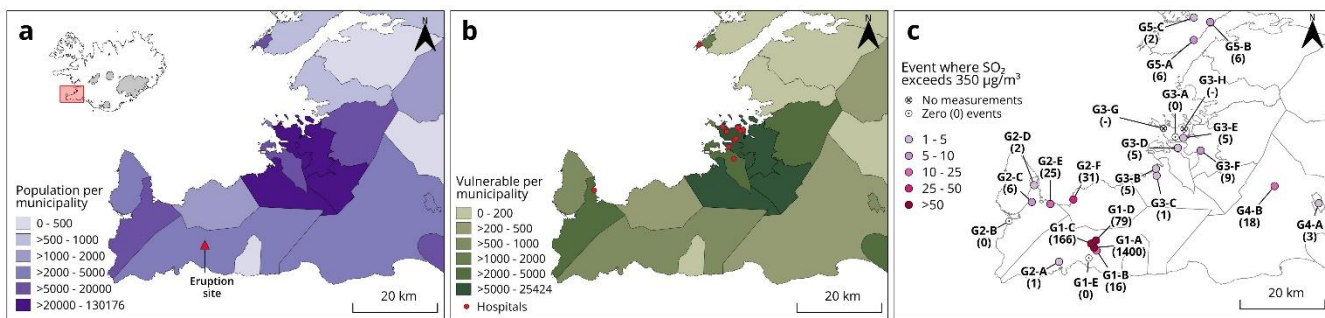
### 3.5 Potential population exposure to volcanic air pollution

#### 3.5.1 Exposure of residents

We considered the frequency of exposure in populated areas to  $\text{SO}_2$  levels above air quality thresholds ( $350 \mu\text{g}/\text{m}^3$  hourly-mean). Evidence-based air quality thresholds for  $\text{PM}_1$  do not yet exist, however, as shown in previous sections (e.g. Figs. 7 and 8), volcanic advection episodes contained  $\text{SO}_2$ ,  $\text{PM}_1$  and  $\text{PM}_{2.5}$  (and to a less significant extent,  $\text{PM}_{10}$ ) and therefore people exposed to elevated levels of volcanic  $\text{SO}_2$  were most likely also exposed to elevated levels of fine PM.



465 Data on the Icelandic population in the year 2020 were obtained from Statistics Iceland (2022) and were considered  
466 representative for 2021. Population data were obtained for each municipality of Iceland, both the total municipality  
467 population as well as population by age demographics. In 2020, Iceland had a population of 369,000. Of the total population,  
468 6% and 15% of the population were in the age groups of  $\leq 4$  and  $\geq 65$  years, respectively, which have been shown to be more  
469 vulnerable to volcanic air pollution (Carlsen et al., 2021b, a). There were 263,000 people, equating to 71% of the total  
470 population, within 50 km of the Fagradalsfjall eruption site where most of the  $\text{SO}_2$  air quality threshold exceedances  
471 occurred. Fig. 9 shows municipality-level population data for this area, number of vulnerable age-group individuals, location  
472 of hospitals, and the number of ID air quality threshold exceedances at monitoring stations.



473 **Figure 9: Potential exposure of the general population of Iceland to above-threshold  $\text{SO}_2$  concentrations ( $350 \mu\text{g}/\text{m}^3$  hourly-mean).** Panel (a): Population map at the municipality level of the densely populated southwestern part of Iceland, including the Reykjavik  
474 capital area (area G3). Population data in this figure for 2020 from Statistics Iceland. Panel (b): Map of potentially vulnerable sub-  
475 populations ( $\leq 4$  years and  $\geq 65$  years of age) in each municipality. Location of hospitals is shown. Panel (c): Number of events  
476 when  $\text{SO}_2$  concentrations exceeded the ID air quality threshold of  $350 \mu\text{g}/\text{m}^3$  hourly-mean during the eruption period as measured  
477 by the monitoring stations (areas G1, G2 and G3). Source and copyright of basemap and cartographic elements: Icelandic Met  
478 Office & Icelandic Institute of Natural History.

480 The capital area had 210,000 residents (60% of the total population), a high density of individuals in the more-vulnerable age  
481 groups and a large number of hospitals (area G3 on Fig. 9). Air quality stations in the densely-populated capital area  
482 recorded between 0 and 9 threshold exceedance events. The fine-scale spatial differences in ground-level pollutant  
483 concentrations (section 3.4) were potentially very important for the total exposure. For example, one of the largest hospitals  
484 in the country was located equidistantly (~2 km) from stations G3-A and G3-E that recorded, respectively, 0 and 5  $\text{SO}_2$   
485 exceedance events, so it is not known how frequently people at the hospital were exposed to above-threshold levels.  
486 Similarly, the hospital closest to the eruption site (20 km distance) was located in between two air quality monitoring stations  
487 (G2-D and G2-E) that recorded very different number of  $\text{SO}_2$  exceedance events - 2 and 25, respectively (Fig. 9).  
488 With respect to nationwide public health impacts, it was fortunate that the volcanic pollutants were predominantly  
489 transported to the north and northwest of the eruption site, likely reducing the number of  $\text{SO}_2$  pollution episodes in the  
490 densely-populated capital to the northeast of the eruption site. The most frequent population exposure to potentially  
491 unhealthy levels of  $\text{SO}_2$  occurred predominantly within a 20 km radius of the volcanic eruption site, in the municipalities on  
492 the Reykjanes peninsula, with up to 31 exceedance events (area G2 on Fig. 9). Individuals who spent their working hours at

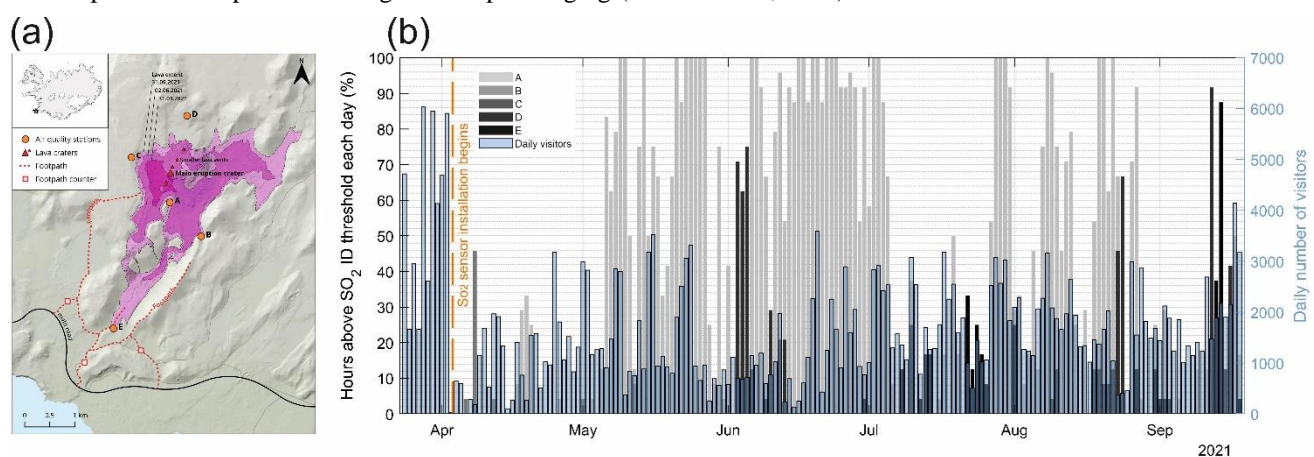


some distance from their place of residence may have been exposed to different levels of volcanic pollution than can be estimated from exposure analysis based on residency. For example, station G2-A in the township of Grindavík recorded one 495 exceedance event, but many of Grindavík's residents worked at Keflavik airport which experienced higher levels of SO<sub>2</sub> pollution (5 events at G2-C, Fig. 9). The reverse may have applied for those residents of Vogar (station G2-E, 25 events) who worked in the Reykjavík capital area where a lower number of exceedance events was observed (0-9 events). The estimated exposure of children was likely more accurate than for adults because most children go to schools within walking 500 distance or minimal commuting distance from their homes. The same applies to long-term hospital inpatients.

500 Municipality-level population datasets are relatively easily available and therefore frequently used in population exposure analysis (Caplin et al., 2019). We show that for assessing air pollution exposure even from relatively distal sources, such as this volcanic eruption (20-55 km distance from source to impacted populated areas) there are challenges with using municipality-level population data, as there are important fine-scale variations. Furthermore, even the exceptionally dense- 505 reference grade air quality network in this part of Iceland was unable to fully spatially resolve the pollution dispersion and frequency of above-threshold events.

### 3.5.2 Exposure of eruption site visitors

An interesting aspect of the eruption was that it was generally considered a very positive event by the Icelandic public (Ilyinskaya et al., 2024), and even though it took place in an uninhabited location the site became akin to a densely populated area due to the extremely high number of visitors. A considerable effort was made by the national and local authorities to 510 minimise the risk from volcanic and general outdoor hazards. A network of three footpaths was developed, starting at designated parking areas (Fig. 10a). The footpaths were modified several times over the course of the eruption as the lava field expanded and optimal viewing areas kept changing (Barsotti et al., 2023).



515 **Figure 10: Eruption site visitor numbers 23 March – 19 September 2024 and potential exposure to above-threshold SO<sub>2</sub> concentrations estimated from eruption-site sensor data that were installed in April (stations A, B) and June (stations C, D, E). Panel (a) Topographic map of the Fagradalsfjall eruption site area showing the locations of the eruption craters, and the extent of the lava field throughout the eruption. It also shows the locations of the five G1 SO<sub>2</sub> air quality sensors (A-E), the footpaths which**



were the most likely locations for visitors, and the location of the footpath visitor counters. Panel (b) shows the number of visitors per day, and the number of hours where  $\text{SO}_2$  was above ID air quality threshold ( $350 \mu\text{g}/\text{m}^3$  hourly-mean) at each station. The number of hours is shown as % of day duration ( $n$  of hours/24\*100). Source and copyright of basemap and cartographic elements: 520 Icelandic Met Office & Icelandic Institute of Natural History.

We estimated the number of people who visited the eruption site by using data from automated footpath counters installed by the Icelandic Tourist Board from 24 March 2021, one on each main footpath leading to the eruption site and viewpoints (Fig. 525 10a). The counters were PYRO-Box with an accuracy of 95% and a sensing capacity of 4 m in both directions (Eco Counter, 2021). Although the vast majority of visitors used the footpath network to reach the eruption site and viewpoints, some may 530 have walked outside the bounds of the Eco-Counter instrument range and so were not counted. There was also a number of people who landed at the eruption site on helicopter sightseeing tours who were not counted. Children who were carried, and people with permission to travel by vehicle (such as scientists and rescue teams) were also not included in the count. The visitor numbers used here are therefore a minimum estimate. The data on visitors to the site did not include details of the age 535 demographics and as such no identification of exposure of more-vulnerable age categories could be determined.

During the footpath monitoring period (24 March to 18 September 2021), the site was visited by ~300,000 people, averaging 1,600 visitors per day. The eruption-response  $\text{SO}_2$  air quality sensors (G1) were set up along the same footpaths and we used 535 these measurements to assess the potential exposure levels of the visitors (Fig. 10). This is based on the assumption that the concentrations measured at the stations are representative of the rest of the footpaths and other locations of the eruption site visited by people, and therefore includes considerable error margins. The highest visitor numbers were in the first weeks of the eruption that coincided with Easter vacation period, with a daily average of 3,300 visitors, and a peak of 6,000 visitors on 540 March 28. G1 stations were not set up until 3 April, therefore we have no indication of the potential exposure during the most-frequently visited period. Figure 10b shows the frequency of ID exceedance events ( $350 \mu\text{g}/\text{m}^3$  hourly-mean  $\text{SO}_2$ ) at each of the 5 monitoring stations, and the number of daily visitors counted on the footpaths. The likelihood of exposure to 545 above-threshold  $\text{SO}_2$  was predominantly in the vicinity of station G1-A, which recorded a cumulative total of 1600 hours above the threshold. Station G1-C had the second highest exposure with cumulative total 110 hourly-exceedances. The other three stations recorded relatively low number of exceedances, between 0 and 20 events. G1-C and G1-D were more frequently downwind of the active vents compared to the other G1 stations (wind rose in Fig. B11), and the local-scale topography played a role. In addition, based on our visual observations of this eruption, and comparable fissure eruptions, a 550 plume from a fissure eruption can occasionally collapse and spread laterally. This leads to extremely high concentrations of  $\text{SO}_2$  even at locations upwind of the volcanic vent.

Our estimate of visitors' exposure to above-threshold events is likely a worst-case scenario because of mitigation actions. The visitors were clearly advised to remain upwind of the active craters and the lava field, and the site was staffed by rescue 555 team members and/or rangers carrying hand-held  $\text{SO}_2$  monitors. When  $\text{SO}_2$  concentrations exceeded threshold levels on the sensors, the visitors were urged to move into cleaner air. It is still quite likely that some visitors were exposed to unhealthy levels of  $\text{SO}_2$  because the area was large enough that rangers with hand-held sensors were not near to all visitors and rapid changes in wind direction often brought  $\text{SO}_2$  to areas that had clean air moments before. This is supported by anecdotal



reports in the Icelandic media regarding individuals seeking health care after visiting the eruption site, reportedly feeling unwell from the gas emissions. The footpath network leading to the eruption viewpoints included an elevation ascent of 200 m, so visitors were undergoing physical exertion with elevated breathing and heartrate while they were within 3 km of the eruption. High levels of physical exertion during exposure to air pollution can increase the exposure of the respiratory system which may result in more significant health impacts (Koenig et al., 1983; Qin et al., 2019).

#### 4 Conclusions

The Fagradalsfjall 2021 eruption was the beginning of a prolonged eruptive period on the Reykjanes peninsula, which is ongoing at the time of writing. All investigations into the recent eruptions may prove useful for risk reduction efforts for years, and generations, to come.

Understanding the volcanic air pollution in a uniquely Icelandic event like the Reykjanes Fires has important implications for how we manage and prepare for other eruptions globally. The fine temporal and spatial variability in the volcanic pollution dispersion that we have discovered in this study calls for further investigation in eruptions in Iceland and other areas exposed to volcanic activity.

We show that even the exceptionally-dense reference grade air quality monitoring network in Iceland could not fully resolve the fine spatial fluctuations in volcanic air pollution episodes. We suggest that air quality networks are augmented, for example with well-calibrated lower-cost sensors, so that increased monitoring can be put in place to protect the most vulnerable individuals in the society, such as at schools and hospitals.

570



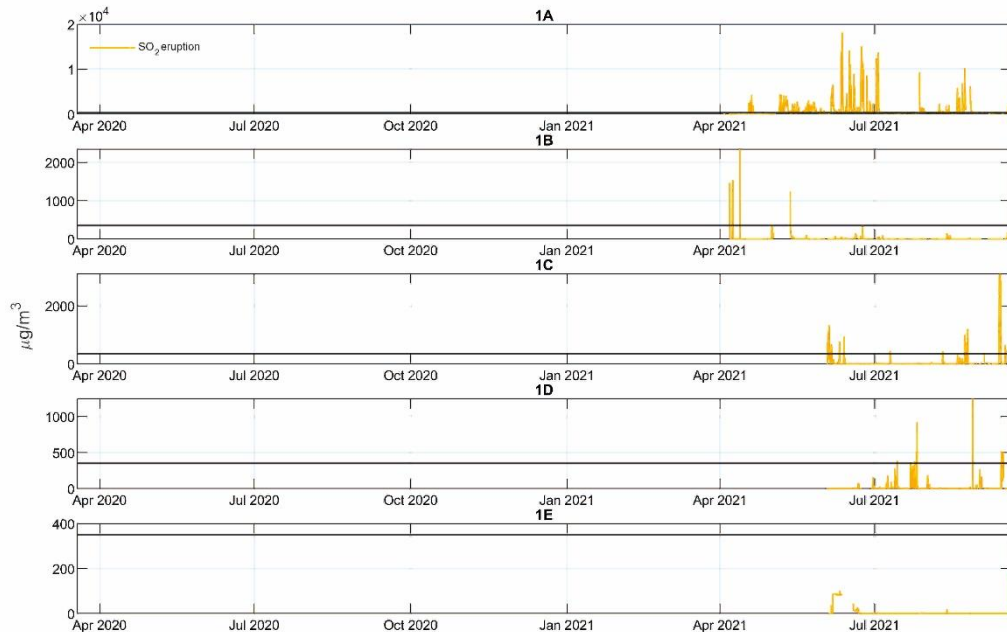
**Table S1**

Excel file ‘Table\_S1.xlsx. Information about instrumentation, data completeness, data exclusion, etc, for each SO<sub>2</sub> and PM monitoring station. Summary statistics for SO<sub>2</sub> (hourly-means), PM<sub>10</sub>, PM<sub>2.5</sub> and PM<sub>1</sub> (daily-means) data during the background and eruption periods. SO<sub>2</sub> concentration data (ug/m<sup>3</sup>) reported to 2 s.f.

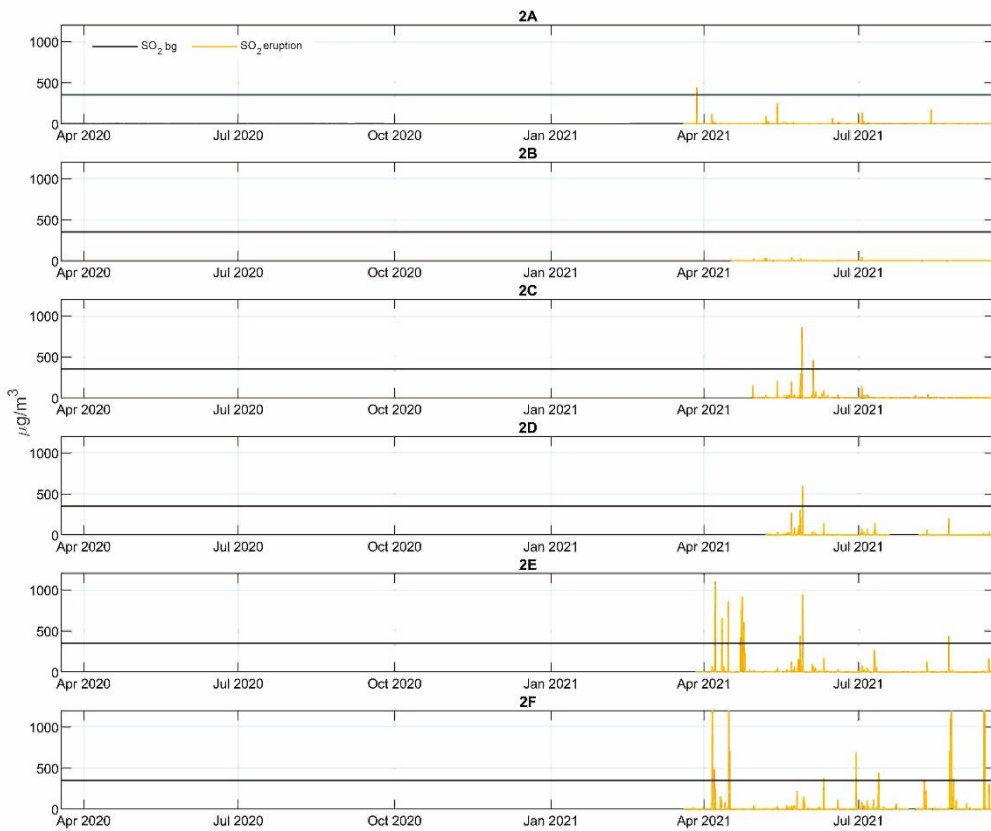
575



## Appendix B.

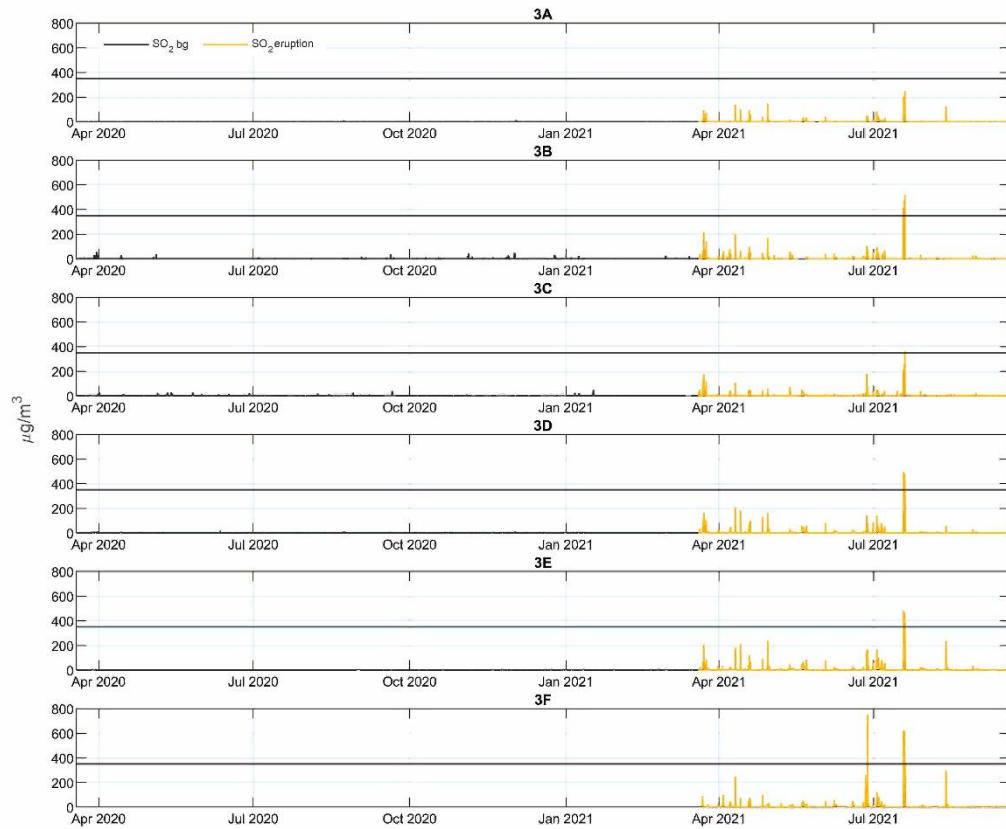


580 Figure B1 Time series of hourly-mean concentrations  $\text{SO}_2$  ( $\mu\text{g}/\text{m}^3$ ), measured by the eruption site stations (G1 A-E) during the 2021 eruption. The stations were not in operation before the eruption and therefore there are no data on pre-eruptive background. The ID air quality threshold of  $350 \mu\text{g}/\text{m}^3$  hourly-mean is shown on all panels with a black horizontal line. Note that the eruption-site sensors have low accuracy and were only used in this study to indicate time periods that were over the ID threshold, the absolute concentration values were not included in the analysis.



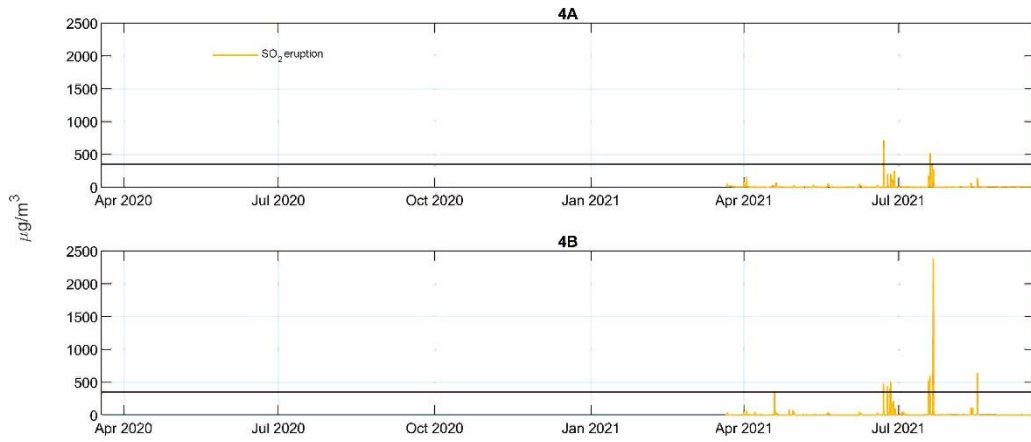
585

**Figure B2** Time series of hourly-mean concentrations  $\text{SO}_2$  ( $\mu\text{g}/\text{m}^3$ ), measured by Reykjanes peninsula reference-grade air quality stations (G2 A-F) during the 2021 eruption and the non-eruptive background in 2020 (bg). The ID air quality threshold of 350  $\mu\text{g}/\text{m}^3$  hourly-mean is shown on all panels with a black horizontal line.



590

**Figure B3** Time series of hourly-mean concentrations  $\text{SO}_2$  ( $\mu\text{g}/\text{m}^3$ ), measured by Reykjavík capital area reference-grade air quality stations (G3 A-F) during the 2021 eruption and the non-eruptive background in 2020 (bg). The ID air quality threshold of 350  $\mu\text{g}/\text{m}^3$  hourly-mean is shown on all panels with a black horizontal line.



595

**Figure B4** Time series of hourly-mean concentrations  $\text{SO}_2$  ( $\mu\text{g}/\text{m}^3$ ), measured in Southwest Iceland by reference-grade air quality stations (G4 A-B) during the 2021 eruption. The stations were not in operation before the eruption and therefore there are no data on pre-eruptive background. The ID air quality threshold of  $350 \mu\text{g}/\text{m}^3$  hourly-mean is shown on all panels with a black horizontal line.

600

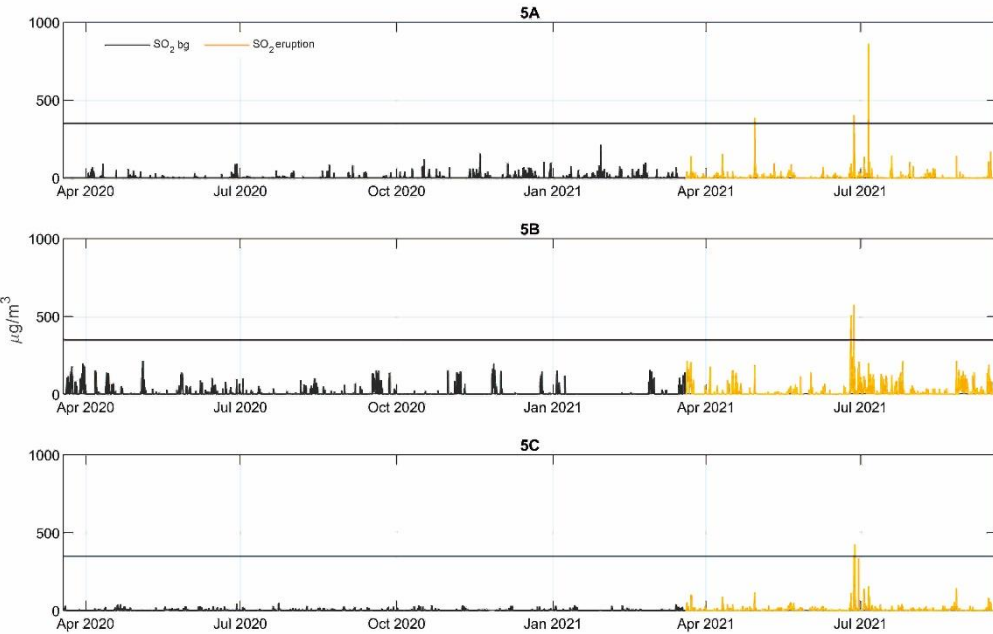


**Figure B5** Time series of hourly-mean concentrations  $\text{SO}_2$  ( $\mu\text{g}/\text{m}^3$ ), measured in Hvalfjörður area by reference-grade air quality stations (G5 A-C) during the 2021 eruption and the non-eruptive background in 2020 (bg). The ID air quality threshold of  $350 \mu\text{g}/\text{m}^3$  hourly-mean is shown on all panels with a black horizontal line.

605

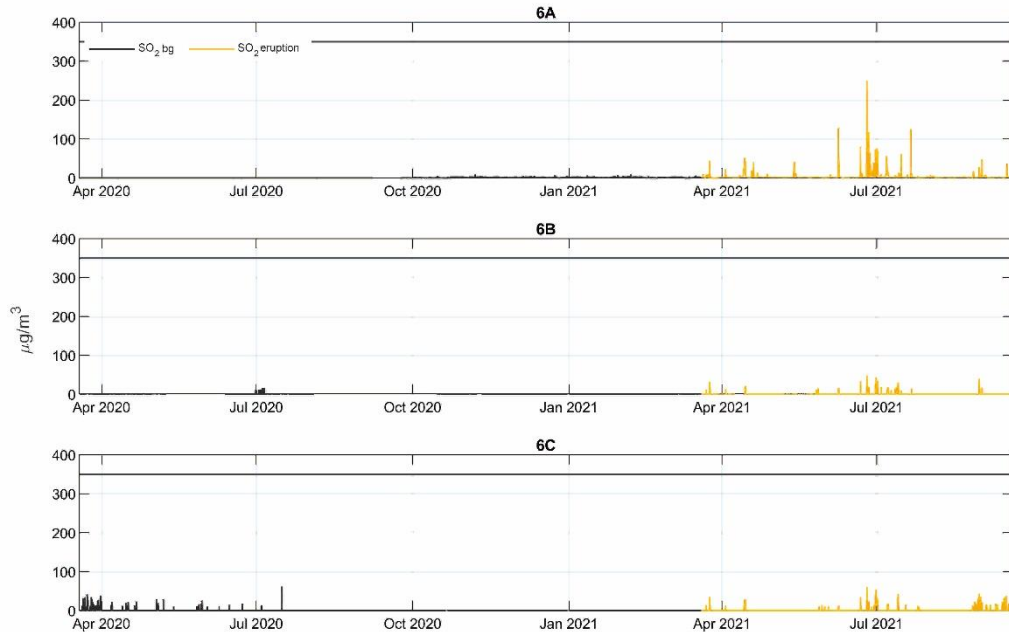


**Figure B6** Time series of hourly-mean concentrations  $\text{SO}_2$  ( $\mu\text{g}/\text{m}^3$ ), measured in North Iceland by reference-grade air quality stations (G6 A-C) during the 2021 eruption and the non-eruptive background in 2020 (bg). The ID air quality threshold of  $350 \mu\text{g}/\text{m}^3$  hourly-mean is shown on all panels with a black horizontal line.

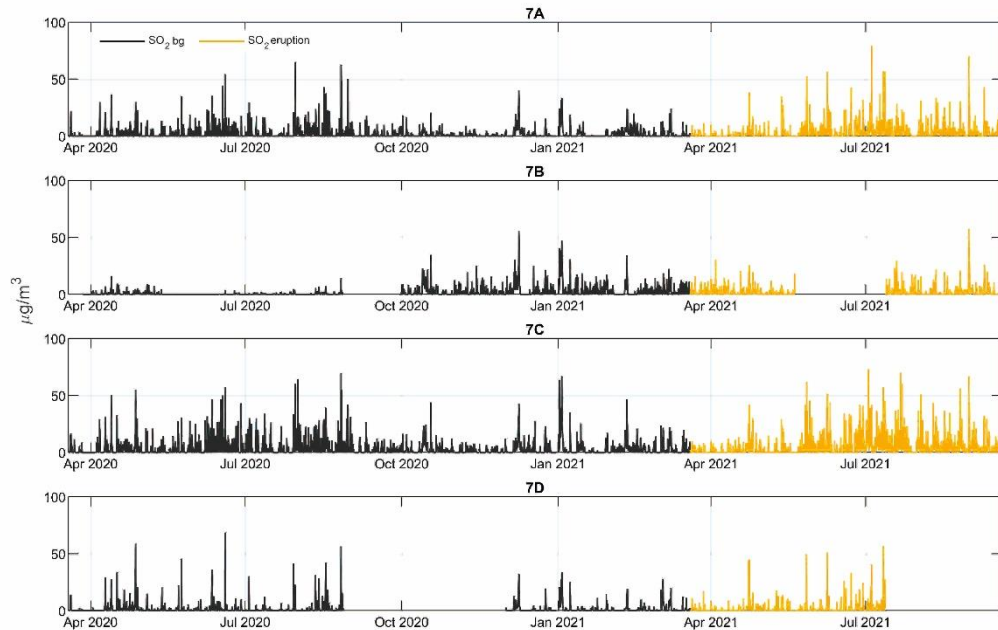


**Figure B7** Time series of hourly-mean concentrations  $\text{SO}_2$  ( $\mu\text{g}/\text{m}^3$ ), measured in East Iceland by reference-grade air quality stations (G7 A-D) during the 2021 eruption and the non-eruptive background in 2020 (bg). The ID air quality threshold of  $350 \mu\text{g}/\text{m}^3$  hourly-mean is shown on all panels with a black horizontal line.

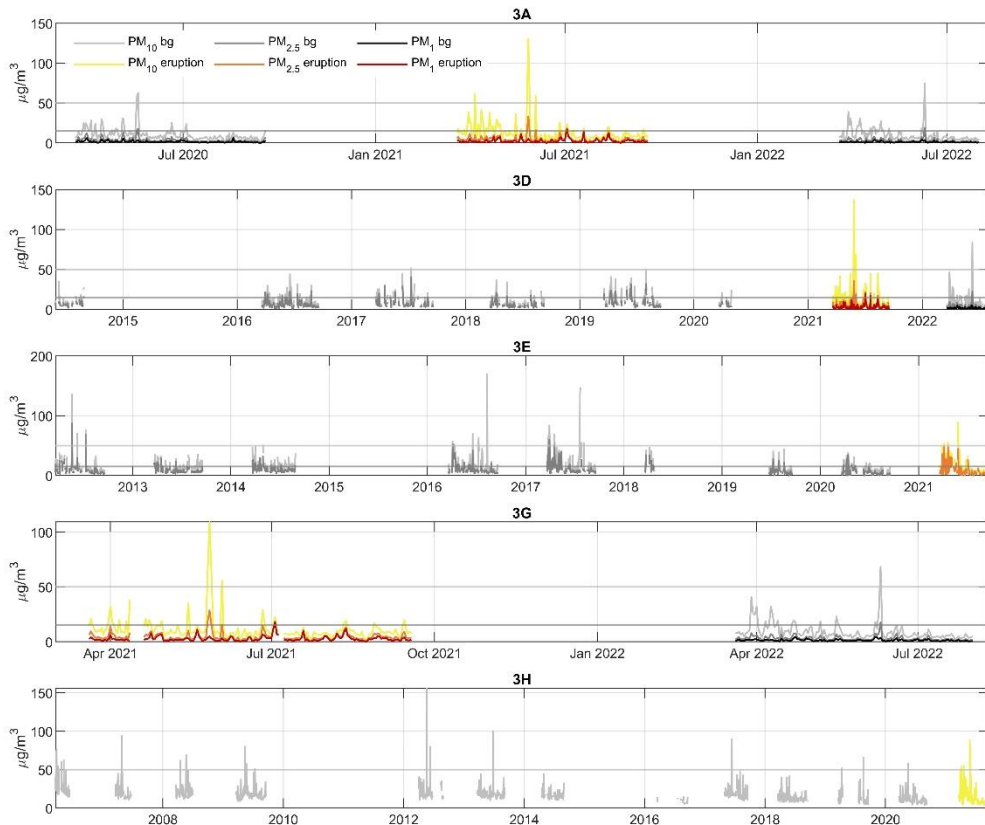
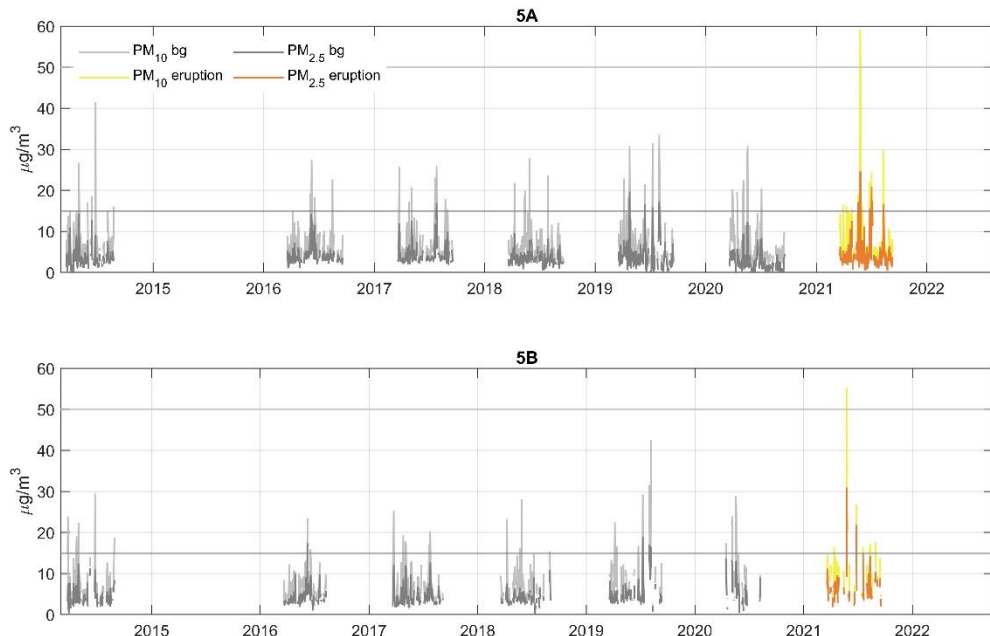


Figure B8 Time series of daily-mean concentrations of  $\text{PM}_{10}$ ,  $\text{PM}_{2.5}$  and  $\text{PM}_1$  ( $\mu\text{g}/\text{m}^3$ ) measured in Reykjavík capital area by reference-grade air quality stations (G3 A, D, E, G, H) during the 2021 eruption and in the non-eruptive background (bg). The amount of non-eruptive background data varies between stations based on their installation date. The figures only include data for the period 19 March 20:00 – 19 September 00:00 UTC in each year, i.e. the period corresponding to the calendar dates and months of the 2021 eruption. See main text for the justification of this approach. The figures show the ID air quality thresholds for  $\text{PM}_{10}$  and  $\text{PM}_{2.5}$  of 50 and 15  $\mu\text{g}/\text{m}^3$  daily-mean, respectively as grey horizontal lines. For  $\text{PM}_1$ , air quality thresholds have not been determined.



625

**Figure B9** Time series of daily-mean concentrations of  $\text{PM}_{10}$ , and  $\text{PM}_{2.5}$  ( $\mu\text{g}/\text{m}^3$ ) measured in Hvalfjörður area by reference-grade air quality stations (G5 A, B) during the 2021 eruption and in the non-eruptive background (bg).  $\text{PM}_1$  was not measured at these stations. The amount of non-eruptive background data varies between stations based on their installation date. The figures only include data for the period 19 March 20:00 – 19 September 00:00 UTC in each year, i.e. the period corresponding to the calendar dates and months of the 2021 eruption. See main text for the justification of this approach. The figures show the ID air quality thresholds for  $\text{PM}_{10}$  and  $\text{PM}_{2.5}$  of 50 and 15  $\mu\text{g}/\text{m}^3$  daily-mean, respectively as grey horizontal lines.

630

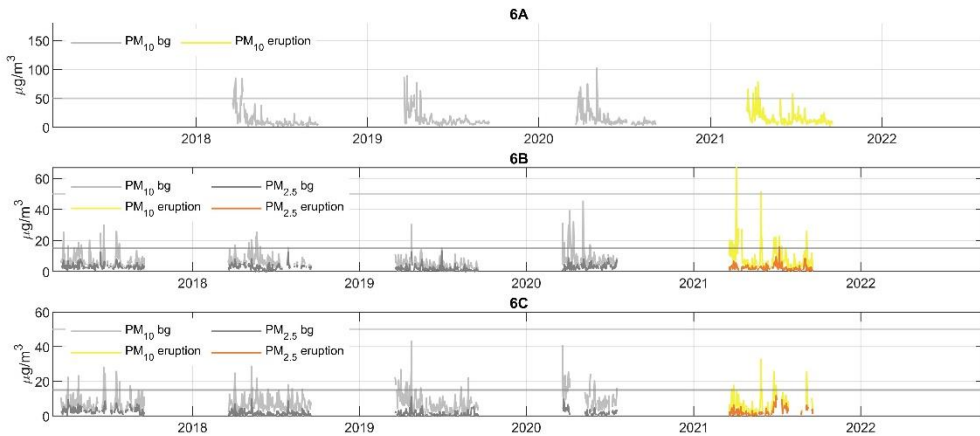
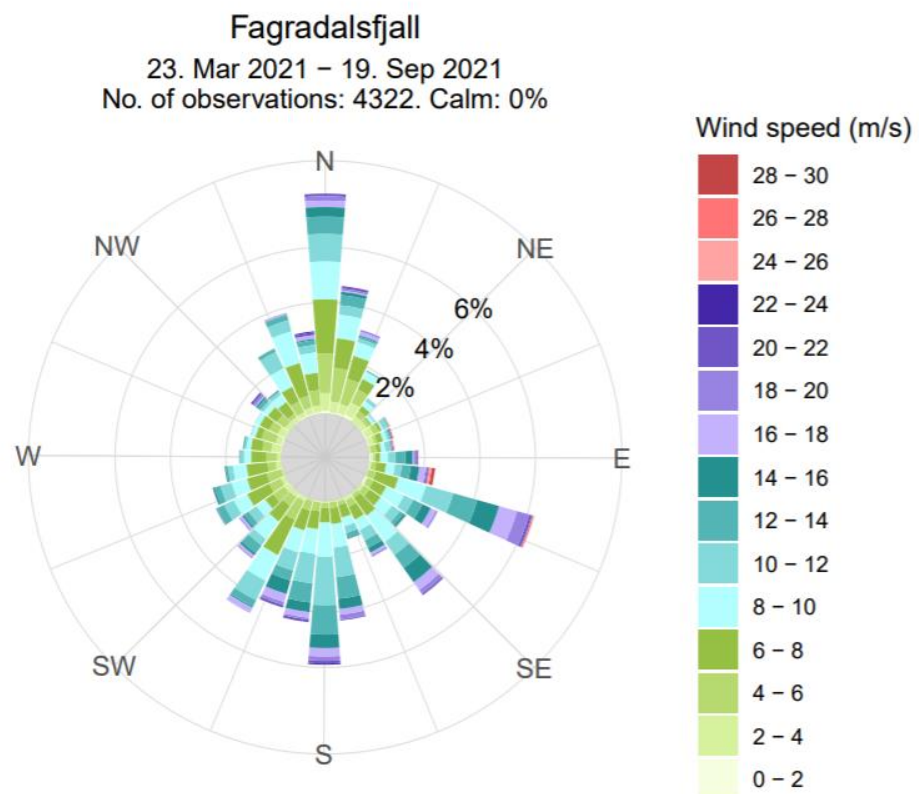


**Figure B10** Time series of daily-mean concentrations of  $PM_{10}$ , and  $PM_{2.5}$  ( $\mu\text{g}/\text{m}^3$ ) measured in North Iceland by reference-grade air quality stations (G6 A, B, C) during the 2021 eruption and in the non-eruptive background (bg).  $PM_1$  was not measured at these stations. The figures only include data for the period 19 March 20:00 – 19 September 00:00 UTC in each year, i.e. the period corresponding to the calendar dates and months of the 2021 eruption. See main text for the justification of this approach. The figures show the ID air quality thresholds for  $PM_{10}$  and  $PM_{2.5}$  of 50 and 15  $\mu\text{g}/\text{m}^3$  daily-mean, respectively as grey horizontal lines.

635



640

**Figure B11** Windrose shows wind direction and wind speed measured by Icelandic Meteorological Office weather station at the Fagradalsfjall eruption site 23 March – 19 September 2021.



## 645 Data availability

Full dataset of SO<sub>2</sub>, PM<sub>10</sub>, PM<sub>2.5</sub> and PM<sub>1</sub> concentrations is openly available for download from the Environment Agency of Iceland <https://loftgaedi.is/en>

## Author contributions

RCWW performed the original data analysis and drafted the original manuscript and figures. SB, MAP, TR and AS 650 contributed to data interpretation and manuscript drafting. EI finalised the data analysis, the manuscript and produced Figs. 2-7, 9 and Appendix B B1-B10. RHTH produced Figs. 1, 8, and 9. TH, GMG and MAP designed, built and maintained IMO's measurement and data systems. TJ contributed access to and information on the reference-grade AQ network and quality-controlled data. DF and RHTH led on the ArcGIS ArcMap analysis methodology. GGS supplied the data from footpath counters. All coauthors contributed to draft review and editing.

## 655 Competing interests

The authors declare that they have no conflict of interest.

## Acknowledgements

The authors would like to thank Kristín Björg Ólafsdóttir from the Icelandic Meteorological Office for analysis of wind data and creation of the wind rose in Appendix B Fig. B11.

## 660 Financial support

RCWW is funded by the Leeds-York Natural Environment Research Council (NERC) Doctoral Training Partnership (DTP) NE/L002574/1, in CASE partnership with the Icelandic Meteorological Office. TJR is funded by the ANR Projet de Recherche Collaborative VOLC-HAL-CLIM (Volcanic Halogens: from Deep Earth to Atmospheric Impacts) ANR-18-CE01-0018, and Labex Orléans Labex VOLTAIRE (VOLatils-Terre Atmosphère Interactions-Ressources et 665 Environnement, ANR-10-LABX-100-0). EI acknowledges NERC Centre for Observation and Modelling of Earthquakes, Volcanoes and Tectonics (COMET+), a partnership between UK Universities and the British Geological Survey; NERC Highlight Topic V-PLUS NE/S00436X/1 and NERC Urgency Grant NE/Z000262/1 “Chemistry of emissions at lava-urban interfaces”.



## References

670 Barsotti, S., Parks, M. M., Pfeffer, M. A., Óladóttir, B. A., Barnie, T., Titos, M. M., Jónsdóttir, K., Pedersen, G. B. M., Hjartardóttir, Á. R., Stefansdóttir, G., Johannsson, T., Arason, P., Gudmundsson, M. T., Oddsson, B., Þrastarson, R. H., Ófeigsson, B. G., Vogfjörd, K., Geirsson, H., Hjörvar, T., von Löwis, S., Petersen, G. N., and Sigurðsson, E. M.: The eruption in Fagradalsfjall (2021, Iceland): how the operational monitoring and the volcanic hazard assessment contributed to its safe access, *Nat. Hazards*, <https://doi.org/10.1007/s11069-022-05798-7>, 2023.

675 Butwin, M. K., von Löwis, S., Pfeffer, M. A., and Thorsteinsson, T.: The effects of volcanic eruptions on the frequency of particulate matter suspension events in Iceland, *J. Aerosol Sci.*, 128, 99–113, 2019.

Caplin, A., Ghandehari, M., Lim, C., Glimcher, P., and Thurston, G.: Advancing environmental exposure assessment science to benefit society, *Nat. Commun.*, 10, 1236, <https://doi.org/10.1038/s41467-019-09155-4>, 2019.

680 Carlsen, H. K. and Thorsteinsson, T.: Associations between PM10 from Traffic, Resuspension, Sand Storms and Volcanic Sources and Asthma Drugs Dispensing, In Review, <https://doi.org/10.21203/rs.3.rs-1017409/v1>, 2021.

Carlsen, H. K., Ilyinskaya, E., Baxter, P. J., Schmidt, A., Thorsteinsson, T., Pfeffer, M. A., Barsotti, S., Dominici, F., Finnbjørnsdóttir, R. G., Jóhannsson, T., Aspelund, T., Gislason, T., Valdimarsdóttir, U., Briem, H., and Gudnason, T.: Increased respiratory morbidity associated with exposure to a mature volcanic plume from a large Icelandic fissure eruption, *Nat. Commun.*, 12, 2161, <https://doi.org/10.1038/s41467-021-22432-5>, 2021a.

685 Carlsen, H. K., Valdimarsdóttir, U., Briem, H., Dominici, F., Finnbjørnsdóttir, R. G., Jóhannsson, T., Aspelund, T., Gislason, T., and Gudnason, T.: Severe volcanic  $\text{CO}_2$  exposure and respiratory morbidity in the Icelandic population—a register study, *Environ. Health*, 20, 1–12, 2021b.

690 Chen, G., Li, S., Zhang, Y., Zhang, W., Li, D., Wei, X., He, Y., Bell, M. L., Williams, G., Marks, G. B., and others: Effects of ambient PM<sub>1</sub> air pollution on daily emergency hospital visits in China: an epidemiological study, *Lancet Planet. Health*, 1, e221–e229, 2017.

Crawford, B., Hagan, D. H., Grossman, I., Cole, E., Holland, L., Heald, C. L., and Kroll, J. H.: Mapping pollution exposure and chemistry during an extreme air quality event (the 2018 Kīlauea eruption) using a low-cost sensor network, *Proc. Natl. Acad. Sci.*, 118, 2021.

695 Crilley, L. R., Shaw, M., Pound, R., Kramer, L. J., Price, R., Young, S., Lewis, A. C., and Pope, F. D.: Evaluation of a low-cost optical particle counter (Alphasense OPC-N2) for ambient air monitoring, *Atmospheric Meas. Tech.*, 709–720, 2018.

Eco Counter: PYRO-Box, <https://www.eco-counter.com/products/pyro-range-pyro-box>, 2021.

Freire, S., Florczyk, A. J., Pesaresi, M., and Sliuzas, R.: An Improved Global Analysis of Population Distribution in Proximity to Active Volcanoes, 1975–2015, *ISPRS Int. J. Geo-Inf.*, 8, 341, <https://doi.org/10.3390/ijgi8080341>, 2019.

700 Gíslason, S. R., Stefánsdóttir, G., Pfeffer, M. A., Barsotti, S., Jóhannsson, Th., Galeczka, I., Bali, E., Sigmarsdóttir, O., Stefánsson, A., Keller, N. S., Sigurdsson, Á., Bergsson, B., Galle, B., Jacobo, V. C., Arellano, S., Aiuppa, A., Jónasdóttir, E. B., Eiríksdóttir, E. S., Jakobsson, S., Guðfinnsson, G. H., Halldórsson, S. A., Gunnarsson, H., Haddadi, B., Jónsdóttir, I., Thordarson, Th., Riishuus, M., Högnadóttir, Th., Dürig, T., Pedersen, G. B. M., Höskuldsson, Á., and Gudmundsson, M. T.: Environmental pressure from the 2014–15 eruption of Bárðarbunga volcano, Iceland, *Geochem. Perspect. Lett.*, 84–93, <https://doi.org/10.7185/geochemlet.1509>, 2015.



705 705 Green, J. R., Fiddler, M. N., Holloway, J. S., Fibiger, D. L., McDuffie, E. E., Campuzano-Jost, P., Schroder, J. C., Jimenez, J. L., Weinheimer, A. J., Aquino, J., and others: Rates of wintertime atmospheric  $\text{CeSO}_2$  oxidation based on aircraft observations during clear-sky conditions over the eastern United States, *J. Geophys. Res. Atmospheres*, 124, 6630–6649, 2019.

710 Icelandic Directive: Reglugerð um brennisteinsdíoxíð, köfnunarefnisdíoxíð og köfnunarefnisoxíð, bensen, kolsýring, svifryk og blý í andrúmsloftinu, B-Deild, Nr.920, 2016.

Ilyinskaya, E., Schmidt, A., Mather, T. A., Pope, F. D., Witham, C., Baxter, P., Jóhannsson, T., Pfeffer, M., Barsotti, S., Singh, A., Sanderson, P., Bergsson, B., McCormick Kilbride, B., Donovan, A., Peters, N., Oppenheimer, C., and Edmonds, M.: Understanding the environmental impacts of large fissure eruptions: Aerosol and gas emissions from the 2014–2015 Holuhraun eruption (Iceland), *Earth Planet. Sci. Lett.*, 472, 309–322, <https://doi.org/10.1016/j.epsl.2017.05.025>, 2017.

715 715 Ilyinskaya, E., Mason, E., Wieser, P. E., Holland, L., Liu, E. J., Mather, T. A., Edmonds, M., Whitty, R. C. W., Elias, T., Nadeau, P. A., Schneider, D., McQuaid, J. B., Allen, S. E., Harvey, J., Oppenheimer, C., Kern, C., and Damby, D.: Rapid metal pollutant deposition from the volcanic plume of Kīlauea, Hawai'i, *Commun. Earth Environ.*, 2, 1–15, <https://doi.org/10.1038/s43247-021-00146-2>, 2021.

720 720 Ilyinskaya, E., Snæbjarnarson, V., Carlsen, H. K., and Oddsson, B.: Brief communication: Small-scale geohazards cause significant and highly variable impacts on emotions, *Nat. Hazards Earth Syst. Sci.*, 24, 3115–3128, <https://doi.org/10.5194/nhess-24-3115-2024>, 2024.

Koenig, J. Q., Pierson, W. E., and Horike, M.: The effects of inhaled sulfuric acid on pulmonary function in adolescent asthmatics, *Am. Rev. Respir. Dis.*, 128, 221–225, <https://doi.org/10.1164/arrd.1983.128.2.221>, 1983.

725 725 Martin, R. S., Ilyinskaya, E., Sawyer, G. M., Tsanev, V. I., and Oppenheimer, C.: A re-assessment of aerosol size distributions from Masaya volcano (Nicaragua), *Atmos. Environ.*, 45, 547–560, <https://doi.org/doi:10.1016/j.atmosenv.2010.10.049>, 2011.

Mason, E., Wieser, P. E., Liu, E. J., Edmonds, M., Ilyinskaya, E., Whitty, R. C. W., Mather, T. A., Elias, T., Nadeau, P. A., Wilkes, T. C., McGonigle, A. J. S., Pering, T. D., Mims, F. M., Kern, C., Schneider, D. J., and Oppenheimer, C.: Volatile metal emissions from volcanic degassing and lava–seawater interactions at Kīlauea Volcano, Hawai'i, *Commun. Earth Environ.*, 2, 1–16, <https://doi.org/10.1038/s43247-021-00145-3>, 2021.

Pattantyus, A. K., Businger, S., and Howell, S. G.: Review of sulfur dioxide to sulfate aerosol chemistry at Kīlauea Volcano, Hawai'i, *Atmos. Environ.*, 185, 262–271, <https://doi.org/10.1016/j.atmosenv.2018.04.055>, 2018.

730 730 Pfeffer, M. A., Arellano, S., Barsotti, S., Petersen, G. N., Barnie, T., Ilyinskaya, E., Hjörvar, T., Bali, E., Pedersen, G. B. M., Guðmundsson, G. B., Vogfjorð, K., Ranta, E. J., Óladóttir, B. A., Edwards, B. A., Moussallam, Y., Stefánsson, A., Scott, S. W., Smekens, J.-F., Varnam, M., and Titos, M.: SO<sub>2</sub> emission rates and incorporation into the air pollution dispersion forecast during the 2021 eruption of Fagradalsfjall, Iceland, *J. Volcanol. Geotherm. Res.*, 449, 108064, <https://doi.org/10.1016/j.jvolgeores.2024.108064>, 2024.

Qin, F., Yang, Y., Wang, S., Dong, Y., Xu, M., Wang, Z., and Zhao, J.: Exercise and air pollutants exposure: A systematic review and meta-analysis, *Life Sci.*, 218, 153–164, <https://doi.org/10.1016/j.lfs.2018.12.036>, 2019.

740 740 Schmidt, A., Leadbetter, S., Theys, N., Carboni, E., Witham, C. S., Stevenson, J. A., Birch, C. E., Thordarson, T., Turnock, S., Barsotti, S., Delaney, L., Feng, W., Grainger, R. G., Hort, M. C., Höskuldsson, Á., Ialongo, I., Ilyinskaya, E., Jóhannsson, T., Kenny, P., Mather, T. A., Richards, N. A. D., and Shepherd, J.: Satellite detection, long-range transport and air quality



impacts of volcanic sulfur dioxide from the 2014–15 flood lava eruption at Bárðarbunga (Iceland), *J. Geophys. Res. Atmospheres*, 2015JD023638, <https://doi.org/10.1002/2015JD023638>, 2015.

745 Siebert, L., Cottrell, E., Venzke, E., and Andrews, B.: Chapter 12 - Earth's Volcanoes and Their Eruptions: An Overview, in: The Encyclopedia of Volcanoes (Second Edition), edited by: Sigurdsson, H., Academic Press, Amsterdam, 239–255, <https://doi.org/10.1016/B978-0-12-385938-9.00012-2>, 2015.

750 Stewart, C., Damby, D. E., Horwell, C. J., Elias, T., Ilyinskaya, E., Tomašek, I., Longo, B. M., Schmidt, A., Carlsen, H. K., Mason, E., Baxter, P. J., Cronin, S., and Witham, C.: Volcanic air pollution and human health: recent advances and future directions, *Bull. Volcanol.*, 84, 11, <https://doi.org/10.1007/s00445-021-01513-9>, 2021.

Wang, Y., Guo, J., Wang, T., Ding, A., Gao, J., Zhou, Y., Collett, J. L., and Wang, W.: Influence of regional pollution and sandstorms on the chemical composition of cloud/fog at the summit of Mt. Taishan in northern China, *Atmospheric Res.*, 99, 434–442, <https://doi.org/10.1016/j.atmosres.2010.11.010>, 2011.

755 Whitty, R., Pfeffer, M., Ilyinskaya, E., Roberts, T., Schmidt, A., Barsotti, S., Strauch, W., Crilley, L., Pope, F., Bellanger, H., Mendoza, E., Mather, T., Liu, E., Peters, N., Taylor, I., Francis, H., Leiva, X. H., Lynch, D., Nobert, S., and Baxter, P.: Effectiveness of low-cost air quality monitors for identifying volcanic SO<sub>2</sub> and PM downwind from Masaya volcano, Nicaragua, *Volcanica*, 5, 33–59, <https://doi.org/10.30909/vol.05.01.3359>, 2022.

760 Whitty, R. C. W., Ilyinskaya, E., Mason, E., Wieser, P. E., Liu, E. J., Schmidt, A., Roberts, T., Pfeffer, M. A., Brooks, B., Mather, T. A., Edmonds, M., Elias, T., Schneider, D. J., Oppenheimer, C., Dybwad, A., Nadeau, P. A., and Kern, C.: Spatial and Temporal Variations in SO<sub>2</sub> and PM<sub>2.5</sub> Levels Around Kīlauea Volcano, Hawai'i During 2007–2018, *Front. Earth Sci.*, 8, <https://doi.org/10.3389/feart.2020.00036>, 2020.

World Health Organization: WHO global air quality guidelines: particulate matter (PM<sub>2.5</sub> and PM<sub>10</sub>), ozone, nitrogen dioxide, sulfur dioxide and carbon monoxide, World Health Organization, xxi, 267 pp., 2021.

765 Yang, M., Chu, C., Bloom, M. S., Li, S., Chen, G., Heinrich, J., Markevych, I., Knibbs, L. D., Bowatte, G., Dharmage, S. C., and others: Is smaller worse? New insights about associations of PM<sub>1</sub> and respiratory health in children and adolescents, *Environ. Int.*, 120, 516–524, 2018.